Photochemical Synthesis of Pd Nanocatalysts Stabilized by Biomass-Derived Polymers: From Colloidal to Supported Systems in Batch and Flow

Irina Della-Cagnoletta,[a,b] Silvia M. Soria-Castro,[a,b*], Fabrizio Politano[a,b], Sandra E. Martín,[a,b] Paula M. Uberman.[a,b,*] and Gabriela Oksdath-Mansilla,[a,b,*]

[a] Universidad Nacional de Córdoba, Facultad de Ciencias Químicas, Departamento de Química Orgánica, Haya de la Torre y Medina Allende. Edificio Ciencias 2. Ciudad Universitaria X5000HUA, Córdoba, Argentina.

[b] Instituto de Investigaciones en Fisicoquímica de Córdoba-INFIQC-CONICET-Universidad Nacional de Córdoba, Haya de la Torre y Medina Allende. Edificio Ciencias 2. Ciudad Universitaria X5000HUA, Córdoba, Argentina

E-mail addresses:

* Silvia M. Soria-Castro (corresponding author): ssoriacastro@unc.edu.ar

Address: Haya de la Torre y Medina Allende. Edificio Ciencias 2. Ciudad Universitaria X5000HUA, Córdoba, Argentina. Telephone/FAX: +54 351 5353865.

*Gabriela Oksdath-Mansilla (corresponding author): gabriela.oksdath@unc.edu.ar

Address: Haya de la Torre y Medina Allende. Edificio Ciencias 2. Ciudad Universitaria X5000HUA, Córdoba, Argentina. Telephone/FAX: +54 351 5353865.

*Paula M. Uberman (corresponding author): paula.uberman@unc.edu.ar.

Address: Haya de la Torre y Medina Allende. Edificio Ciencias 2. Ciudad Universitaria X5000HUA, Córdoba, Argentina. Telephone/FAX: +54 351 5353865.

Table of contents

1. General materials and methods	**S3**
2. Photochemical reactors	**S5**
3. Synthesis of colloidal Pd-PVP and Pd-CMC NPs	**S5**
4. Characterization of colloidal Pd-NPs and control reactions	**S6**
5. Characterization of colloidal Pd-NPs by TEM and UV-Vis spectroscopy	**S7**
6. Characterization by FT-IR, ^{1}H NMR and DLS analysis of colloidal Pd-CMC NPs	**S10**
7. Representative procedure for the Suzuki-Miyaura cross-coupling reaction catalyzed by colloidal Pd-NPs	**S12**
8. Synthesis and characterization of SiO_2 nanospheres functionalized with APTES (SNPs) as support	**S15**
9. Methodology approaches for the preparation of supported Pd-NPs onto SNPs and characterization	**S16**
10. Representative procedure for the Suzuki-Miyaura cross-coupling reaction catalyzed by supported Pd nanocatalysts	**S23**
11. Representative procedure for the Suzuki-Miyaura cross-coupling with different aryl halides and phenylboronic acids	**S23**
12. Representative procedure for recycling experiment with supported Pd-NPs on SNPs	**S25**
13. Characterization data of Suzuki-Miyaura cross-coupling reaction products	**S26**
14. NMR spectra of Suzuki-Miyaura cross-coupling reaction products	**S29**
15. References	**S39**

1. General materials and methods

All chemicals were reagent grade and were used as received from the manufacturer. Palladium (II) chloride ($PdCl_2$, Anedra), hydrochloric acid (HCl 37 % w/w), ammonium hydroxide (NH_4OH, 28 % w/w), trisodium citrate dihydrate (Sigma Aldrich®); disodium oxalate (Sigma Aldrich®), poly(*N*-vinylpyrrolidone) polymer (Mw PVP = 10000 Da), sodium carboxymethylcellulose (Sigma Aldrich®, medium viscosity), tetraethyl orthosilicate (TEOS), (3-aminopropyl)-triethoxysilane (APTES), 4-bromoacetophenone, 4-iodoacetophenone, 4-chloroacetophenone, 4-iodoanisole, 4-bromoanisole, 2-iodoanisole, 4-iodobenzonitrile, 4-bromobenzonitrile, 3-bromoquinoline, phenylboronic acid, 4-fluorophenylboronic acid, K_3PO_4, ethanol 98 % (Porta ®) and anhydrous Na_2SO_4 were used as received. All solvents were analytical grade and distilled before use. H_2PdCl_4 feedstock 2 mM solution was prepared from analytical grade chemicals and Milli-Q-Millipore water. Suzuki-Miyaura cross coupling reactions were carried out under air atmosphere. Silica gel (0.063–0.200 mm) was used in column chromatography.

Photochemical reactions in batch were carried out in scintillation vials equipped with a magnetic bar and sealed with teflon plugs. The mixtures were irradiated with a blue 5 W LED (462 nm) and stirred under argon atmosphere.

Photochemical reactions in flow were carried out in a mesoscale photochemical flow reactor (6.56 mL with 0.75 mm ID FEP-tubing) equipped with a blue-LED reactor (15 x 5 W at 462 nm). A battery-powered magnetic stirrer (Cole-Parmer™) was used for the flow experiments.

The colloidal and supported catalysts were characterized by Transmission Electron Microscopy (TEM) using a TEM Hitachi HT7800 120 kV microscope operating at 80 kV, available at the Centro de Microscopía Electrónica Facultad de Ciencias Médicas, UNC in Córdoba, Argentina. SEM microscopy was performed in a SEM - Zeiss Sigma 360 (Lamarx-UNC). The hydrodynamic apparent diameter (d_H) of the samples were determined by Photon Correlation Spectroscopy (Dynamic Light Scattering, DLS) using a Delsa Nano C instrument (Beckman

Coulter, Osaka, Jp.). Characterization by XRD was performed using a PANalytical X'Pert Pro diffractometer (40 kV, 40 mA) in Bragg–Brentano reflection geometry with Cu Ka radiation (l = 1.5418 A). Data were gathered between 101 and 701 (2y) in steps of 0.02 and a counting time of 24 s. The refinement of the crystal structure was performed by the Rietveld method using the FULLPROF program.

A commercial Thermo Scientific K-Alpha X-ray photoelectron spectrometer (XPS) system (LAMARX, FaMAF-UNC), equipped with a hemispherical energy analyzer and a monochromated X-ray source was used for surveying the photoemission spectra. The base pressure measured in the main chamber was in the low 10-9 mbar range. The photoionization of the samples was induced by monochromatized Al Kα photons at 1486 eV.

Gas chromatographic analysis was performed on a gas chromatograph with a flame ionization detector and equipped with the following columns: HP-5 25 m × 0.20 mm × 0.25 μm column. Gas Chromatographic/Mass Spectrometer analyses were carried out on a GC/MS QP 5050 spectrometer equipped with a VF-5ms, 30 m × 0.25 mm × 0.25 μm column. UV-Vis determinations were performed using a SHIMATZU UV-Vis UV- 1800 series. ^{1}H NMR and ^{13}C NMR were conducted on a High-Resolution Spectrometer Bruker Advance 400. FT-IR spectra were recorded on a Nicolet iN10 IR Microscope (Thermo Scientific).

ICP-MS analysis was performed on an Agilent 7500cx Spectrometer equipped with an Agilent ASX-500 Series autosampler, using argon as carrier gas, available at ICYTAC-CONICET-UNC in Córdoba, Argentina. Pd and Re (185) signals were simultaneously recorded as internal standards for each sample. All aqueous samples were digested before injection using HNO_3 for 18 h at room temperature.

2. Photochemical reactors

(a)

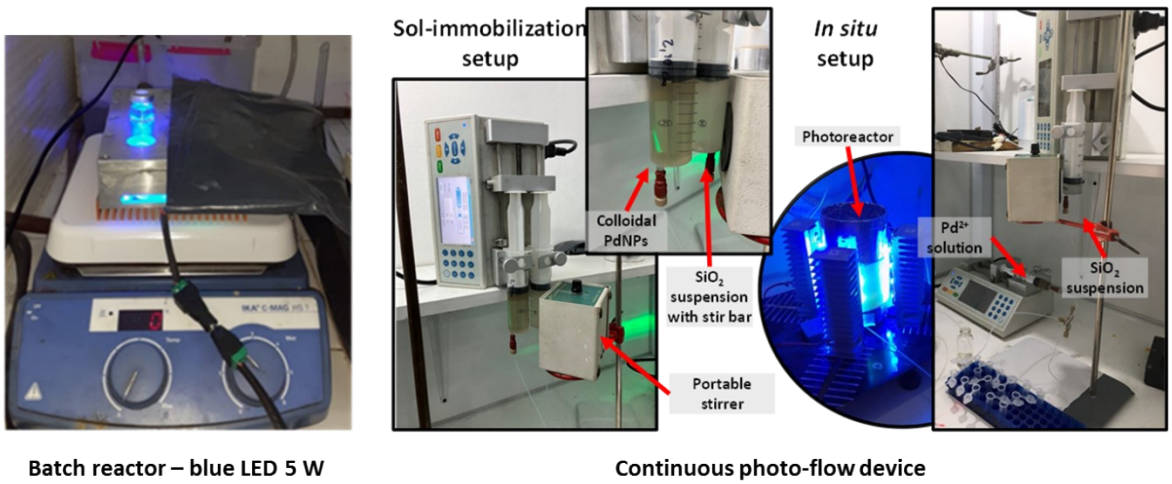

(b)

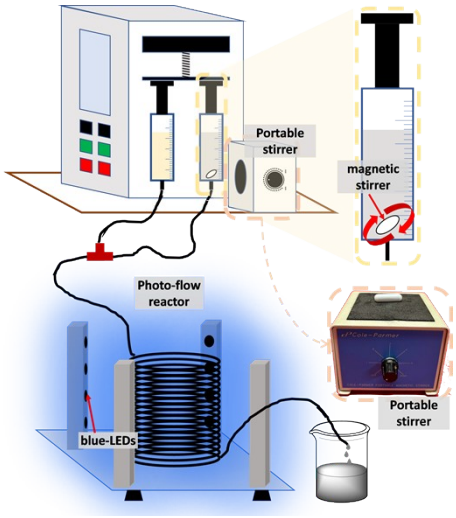

***Figure SI 1**: a) photochemical reactors used in the batch and photo-flow synthesis of Pd NPs with PVP or CMC as stabilizer and in colloidal suspension or supported onto SNPs. b) Schematic representation of the photo-flow continuous setup.*

3. Synthesis of colloidal Pd-PVP and Pd-CMC NPs

In a 10 mL scintillation vial equipped with a magnetic stir bar, 25-100 mg of PVP (0.5-2.0% w/v) or 12.5-50.0 mg of CMC (0.25-1.0% w/v); 29.4 mg of sodium citrate (molar ratio Pd^{2+}/reducing agent 1:10) and 5 mL of a feedstock aqueous solution of H_2PdCl_4 2 mM were placed. When CMC was used as a stabilizing agent, the solution was stirred for 30 min until the polymer was

fully hydrated. The vial was sealed and high purity Ar bubbled for 5 min to saturate the solution. Next, the vial was placed into the photochemical reactor and was irradiated under vigorous magnetic stirring until the mixture color changes to dark brown solution. Finally, the vial was opened to the air, and the Pd-PVP or Pd-CMC NPs dispersions were stored in a falcon tube to be used as catalyst solution without further purification.

4. Characterization of colloidal Pd-NPs and control reactions

Average dimensions and shape of Pd-PVP and Pd-CMC NPs were determined by Transmission Electron Microscope (TEM) images. Samples for morphological characterization were prepared by depositing a drop of the colloidal suspension on a 300 mesh formvar-carbon coated copper grid and dried at room temperature. Size distribution of Pd-NPs was established by the average over 100 NPs from different places at each image of all samples. Distribution plots of the size were resolved by fitting data with a Gaussian behavior.

After the synthesis, the colloidal dispersion of Pd-CMC NPs with 0.5% w/v of stabilizer was examined by Dynamic Light Scattering technique (DLS) to determine the hydrodynamic apparent diameter (d_H) of the samples by photon correlation spectroscopy.

FT-IR and ^{1}H NMR spectroscopies were used to assess the composition of the Pd-CMC NPs and analyze the presence of functional groups of the reactants after the synthesis. In both cases, samples were freeze-dried before analysis. D_2O was used as a solvent for the ^{1}H NMR spectroscopy. For FT-IR analysis samples contained in KBr discs were scanned from 400 and 4000 cm^{-1}, and the recording conditions were: normal resolution, sample scan, 64 s^{-1}. The spectra were analyzed using OMNIC 8 software-ThermoFischer.

5. Characterization of colloidal Pd-NPs by TEM and UV-Vis spectroscopy

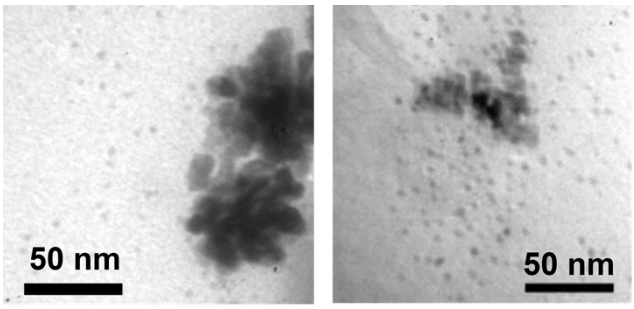

Figure SI 2*. TEM micrographs of Pd-PVP NPs with 0.5 % w/v of stabilizer, showing the presence of aggregates in the sample.*

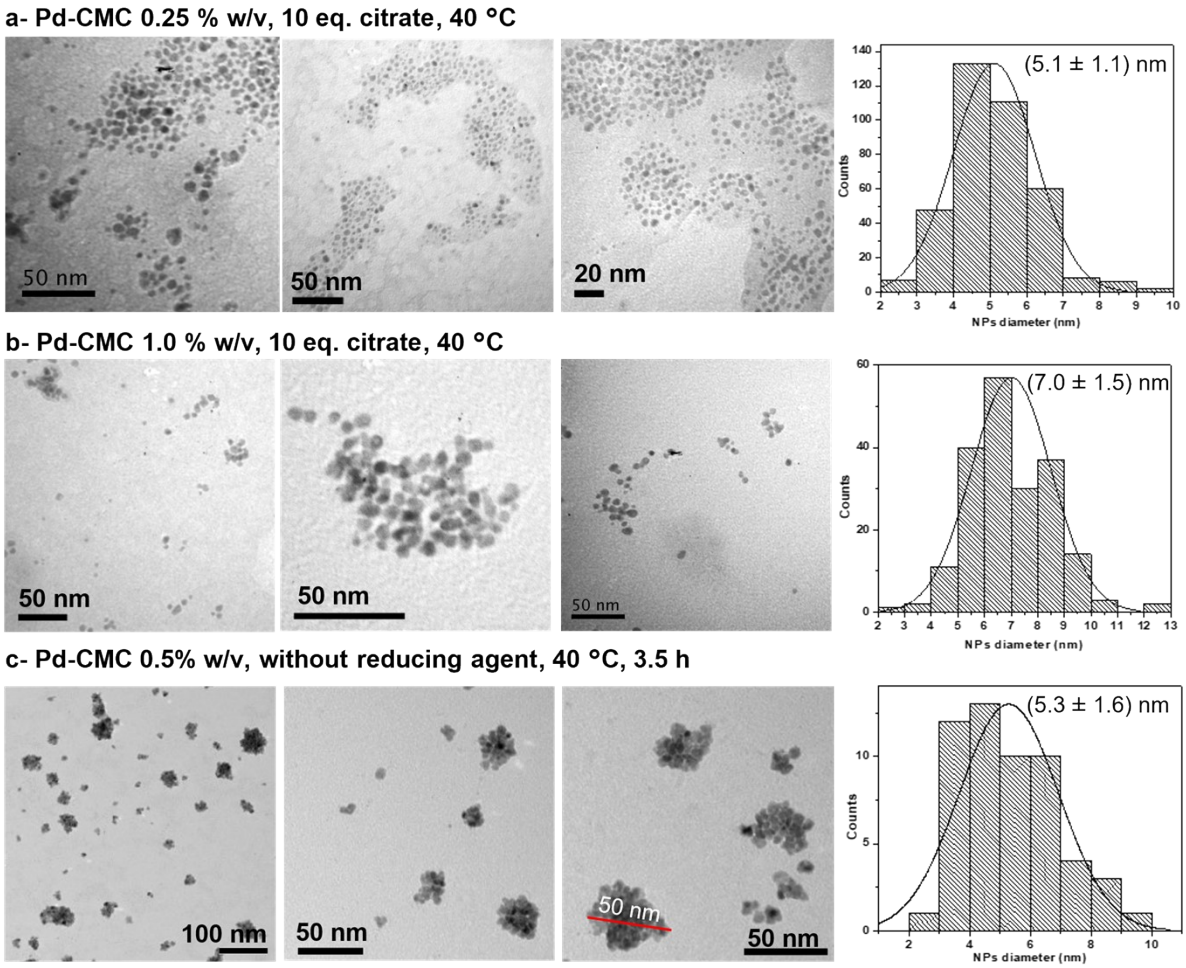

Figure SI 3: TEM micrographs of Pd-CMC NPs prepared with (a) 0.25 % w/v, (b) 1.0 % w/v of stabilizer; (c) without reducing agent. Pd-NPs prepared with 0.25 % w/v and 1.0 % w/v of stabilizers have a spherical morphology and diameters under 10 nm. Large aggregates of particles (~50 nm) were observed in the absence of reducing agent.

Control reactions were performed to assess whether the CMC has an additional effect during the photochemical reduction. For that, we recorded the UV-Vis spectra from 800-250 nm of the following solutions:

- Reaction mixture Pd^{2+} + citrate + CMC (0.5% w/v) without irradiation (dark conditions) for 1.5 hours.

- Reaction mixture Pd^{2+} + CMC (0.5% w/v) without sodium citrate before and after irradiation for 1.5 h and 3.5 h
- H_2PdCl_4 2 mM aqueous solution as a control sample.
- Pd-CMC NPs (0.5% w/v)

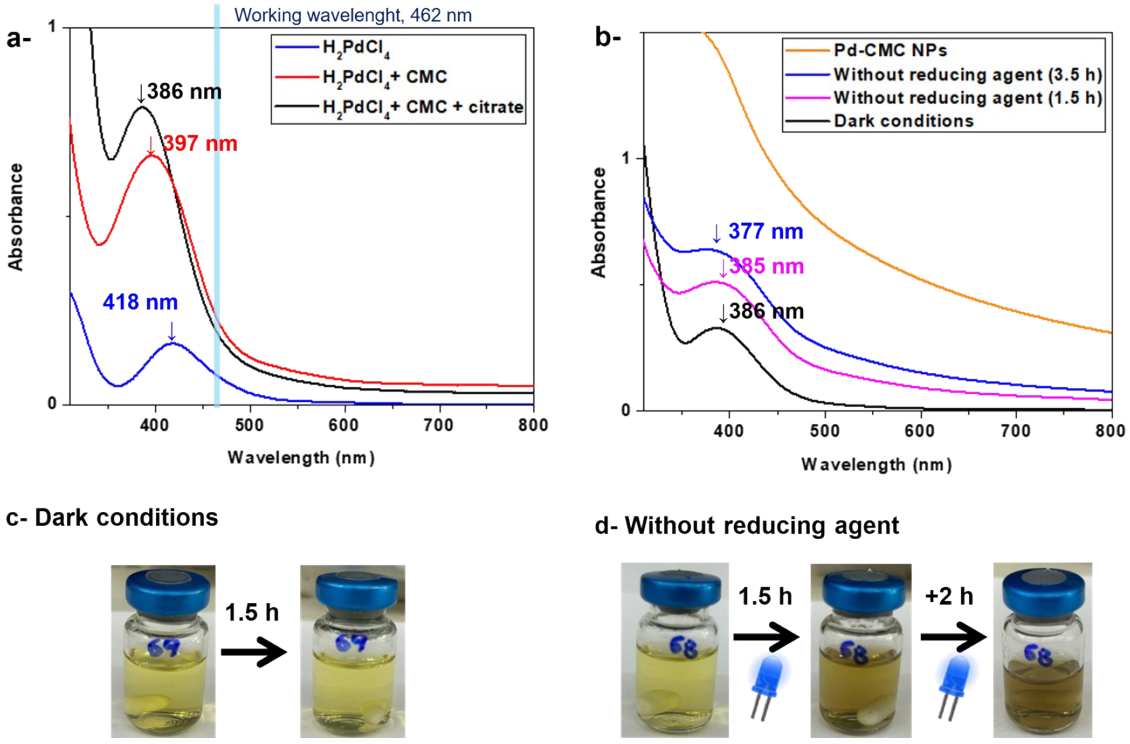

***Figure SI 4**: (a) Optical absorption spectra of H_2PdCl_4 (blue line), H_2PdCl_4+CMC (red line) H_2PdCl_4+CMC+citrate (black line) and absorption peaks. (b) Optical absorption spectra Pd-CMC NPs (0.5 % w/v) (orange line), reaction mixture under dark conditions for 1.5 h (black line) and H_2PdCl_4+CMC (0.5 % w/v) without citrate under irradiation for 1.5 h (pink line) and 3.5 h (blue line). (c) Images of the solutions before and after performing the Pd-CMC NPs synthesis under dark conditions, indicating that the reduction of Pd^{2+} salts does not occur under these conditions. (d) Images of the solutions before and after performing the Pd-CMC NPs synthesis without citrate and at different irradiation times.*

6. Characterization by FT-IR, ^{1}H NMR and DLS analysis of colloidal Pd-CMC NPs

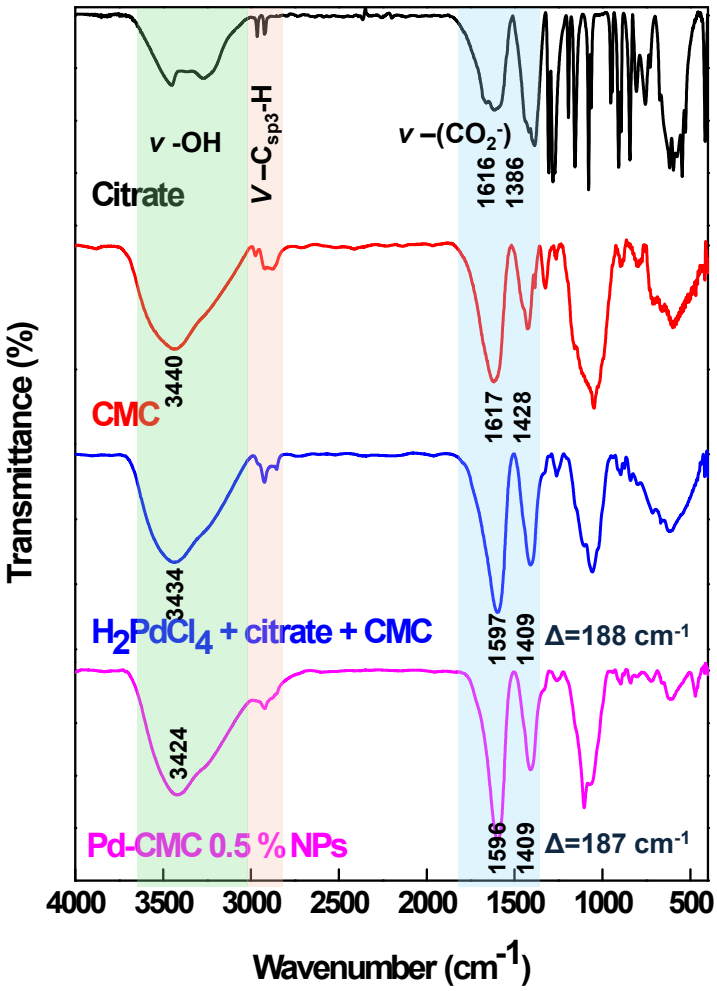

***Figure SI 5**: FT-IR spectra of citrate (black plot), CMC (red plot), and a mixture of H_2PdCl_4 + citrate + CMC 0.5% w/v (before irradiation, blue plot) and Pd-CMC NPs (after irradiation, purple plot).*

In all samples, the bands between 3000-2800 cm^{-1} correspond to the stretching vibration of aliphatic C-H bonds from CMC and citrate (highlighted in orange). In the CMC spectrum, bands at 1617 and 1428 cm^{-1} correspond to the asymmetric and symmetric bands of carboxylate groups (-COONa), and at 1047 cm^{-1} appear the bands of the C-O-C groups.[1] The Δ corresponds to the difference between the asymmetric and symmetric bands of carboxylate groups.

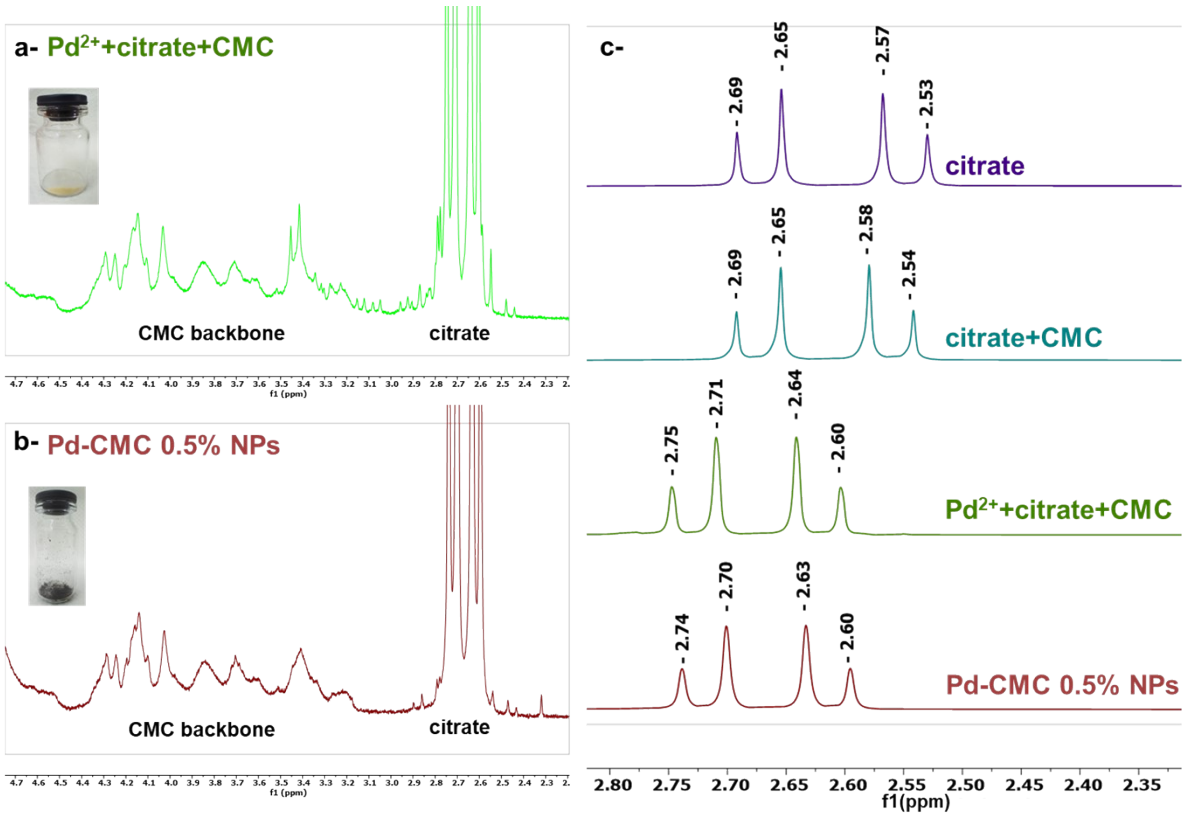

Figure SI 6. *^{1}H NMR spectrum of (a) the reaction mixture of H_2PdCl_4 + citrate + CMC 0.5% w/v and (b) the colloidal suspension of Pd-CMC NPs. In-set shows the color of freeze-dried samples used to measure the spectra. (c) Comparative zoom-in view of the spectra showing the signals of citrate and their chemical shifts in presence of Pd species in the different samples.*

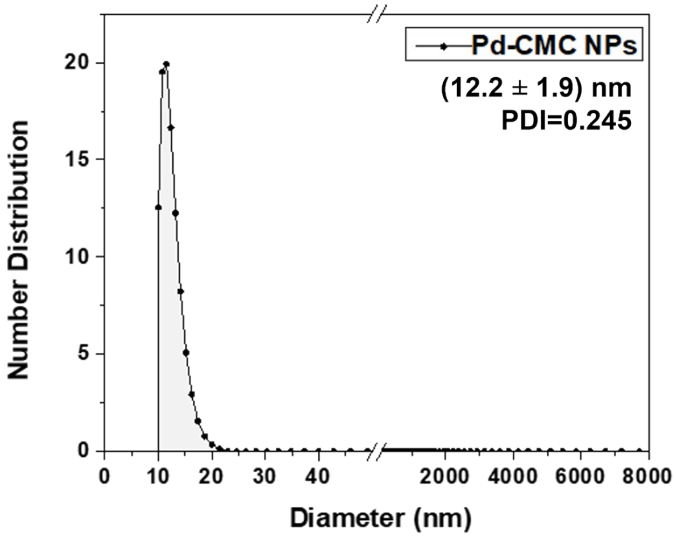

Figure SI 7: *DLS analysis of colloidal Pd-CMC NPs prepared with 0.5% w/v of stabilizer.*

7. Representative procedure for the Suzuki-Miyaura cross-coupling reaction catalyzed by colloidal Pd-NPs

Into a 10 mL tube reaction with a Teflon screw-cap septum equipped with a magnetic stirrer *p*-bromoacetophenone (**1**) (0.25 mmol), phenylboronic acid (**2**) (0.35 mmol) and K_3PO_4 (0.75 mmol) were placed. Then, EtOH (0.5 mL) and water (to obtain a total volume of 1.5 mL taking into account the volume of Pd-NPs solution) were added. At last, the 52 µL of Pd-NPs 2mM (0.04 mol%) was added. The reaction mixture was heated in an oil bath for 1 h. After being cooled to room temperature, the mixture was opened to the air, diluted with water and then extracted three times with ethyl acetate (5 mL each). The biaryl product was purified by silica-gel column chromatography after being dried with anhydrous Na_2SO_4. The product was quantified by GC employing benzophenone as internal standard. The pure product was compared with authentic samples by GC, GC-MS, ^{1}H NMR and ^{13}C NMR as shown in Section 12.

TOF values were calculated as the number of moles of substrate **3a** converted per mol of Pd_{total} per unit time (h), using the following equation 1:

$$TOF = \frac{3a\ mol\ converted}{\left(Pd_{total}\ mol\right) \times\ t} \qquad \text{(eq. 1)}$$

***Table SI 1**: Suzuki-Miyaura cross-coupling reaction catalyzed by Pd-NPs prepared through photochemical reduction with PVP and CMC polymer in different proportions.*

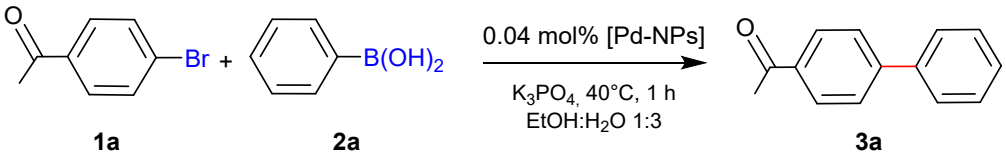

1a **2a** **3a**

Entry	Stabilizer w/v (%)	Yield of 3a (%)[b,c]	TOF (h^{-1}) [c]
1	PVP (2.0 % w/v)	98	2205
2	PVP (1.0 % w/v)	95	2469
3	PVP (0.5 % w/v)	99	2344
5	CMC (1.0 % w/v)	94	1979
6	CMC (0.5 % w/v)	100	2338
7	CMC (0.25 % w/v)	100	2214

a- Reaction conditions: 0.25 mmol **1a**, 0.35 mmol **2a**, 0.75 mmol K_3PO_4, 52 μL of colloidal Pd-NPs, ethanol:water 1:3. b- Quantified by GC analysis with benzophenone as internal standard. c- The yields and TOFs reported represent at least the average of two reactions

***Table SI 2**: Comparison of catalytic activity of Pd-CMC NPs and some selected Pd-based nanocatalysts in the literature for Suzuki-Miyaura cross-coupling reaction between 4-bromoacetophenone (**1a**) and phenylboronic acid (**2a**).*

Catalyst	Catal. load. (mol %)	Reaction medium	Base	Temp (ºC)	Time (h)	TOF (h^{-1})[ref]
Pd-CMC NPs	0.04	EtOH: H_2O	K_3PO_4	40	1	2338 This work
CMC Pd^{II} [b,d]	0.60	EtOH	K_2CO_3	78	0.5	303[2]
Pd NPs[a]	3	H_2O	Na_2CO_3	60	11	3[3]
Pd/C (10 %)[b]	0.5	*i*-PrOH:H_2O	K_3PO_4	r. t.	3	61[4]
PdO/Ce_xO_y	1 mg	EtOH:H_2O	NaOH	70	1	13944[5]
Pd NPs@CS [c]	1	EtOH:H_2O	K_2CO_3	65	3	33[6]
CMC-NHC-Pd[e]	0.8	EtOH:H_2O	K_2CO_3	60	3	62[7]
Chit-Cell/Pd[f]	0.004	Solvent-free	K_2CO_3	50 (MW)	0.08	284375[8]
Pd/HNC[g]	50 mg	H_2O	K_2CO_3	80	8	n.i.[9]
Pd-Fe@Fe_3O_4[h]	0.825 mg	EtOH:H_2O	K_2CO_3	60	2	1239[10]

a- Pd NPs stabilized with proline-based amphiphile PS-750-M. 4-Chlorophenylboronic acid was used. b- 4-Bromobenzaldehyde was used as a substrate. c- Cellulose sponge was used as support. Bromobenzene was used as a substrate. d- Formation of the Pd NPs was detected under the catalytic reaction. e- 4-bromobenzonitrile and 4-fluorophenylboronic acid were used as substrates. f- -bromobenzonitrile and phenylboronic acid were used as substrates. g- 4-Bromotoluene and phenylboronic acid were used as substrates, and TOF value was not informed. h- Magnetic Fe and Pd supported co-catalyst was used. The reaction was carried out under ultrasound conditions and using bromobenzene as substrate.

***Table SI 3:** Suzuki–Miyaura cross-coupling reaction catalyzed by Pd-NPs stabilized with 0.5 % w/v of PVP and CMC for 30 minutes at 30 °C.*

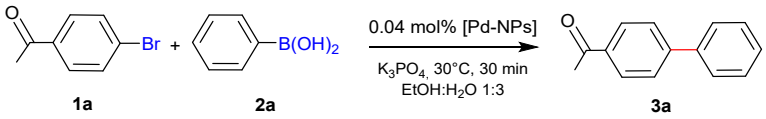

1a **2a** **3a**

Entry	**Catalyst**	**Yield of 3a (%)[b]**	**TOF (h^{-1})**
1	Pd-PVP NPs	61	3126
2	Pd-CMC NPs	68	3733

a- Reaction conditions: 0.25 mmol **1a**, 0.35 mmol **2a**, 0.75 mmol K_3PO_4, 52 μL of colloidal Pd NPs, ethanol:water 1:3. b- Quantified by GC analysis with benzophenone as internal

standard.

8. Synthesis and characterization of SiO_2 nanospheres functionalized with APTES (SNPs) as support

In a 100 mL round-bottom flask equipped with a magnetic stir bar, 60 mL of ethanol and 4.8 mL of NH_4OH aqueous solution (28 % w/w) were placed. After vigorously stirring of the mixture for 5 min, 2.5 mL of TEOS were added. This mixture was stirred for 24 h at room temperature. Then, 200 µL of APTES were added, and the mixture was stirred for another 24 h. For purification of SNPs, the reaction mixture was centrifuged for 8 min at 3500 rpm, the supernatant was discarded, and the white solid was washed with ethanol, sonicated by 5 min and centrifuged again. This procedure was repeated 3 times. Finally, the SNPs were dried under air at room temperature for 24 h. After this procedure, 670 mg of SNPs were recovered to use as a support for the Pd NPs.

The schematic representation of the synthesis and characterization of the SNPs are shown in **Figure SI 8**.

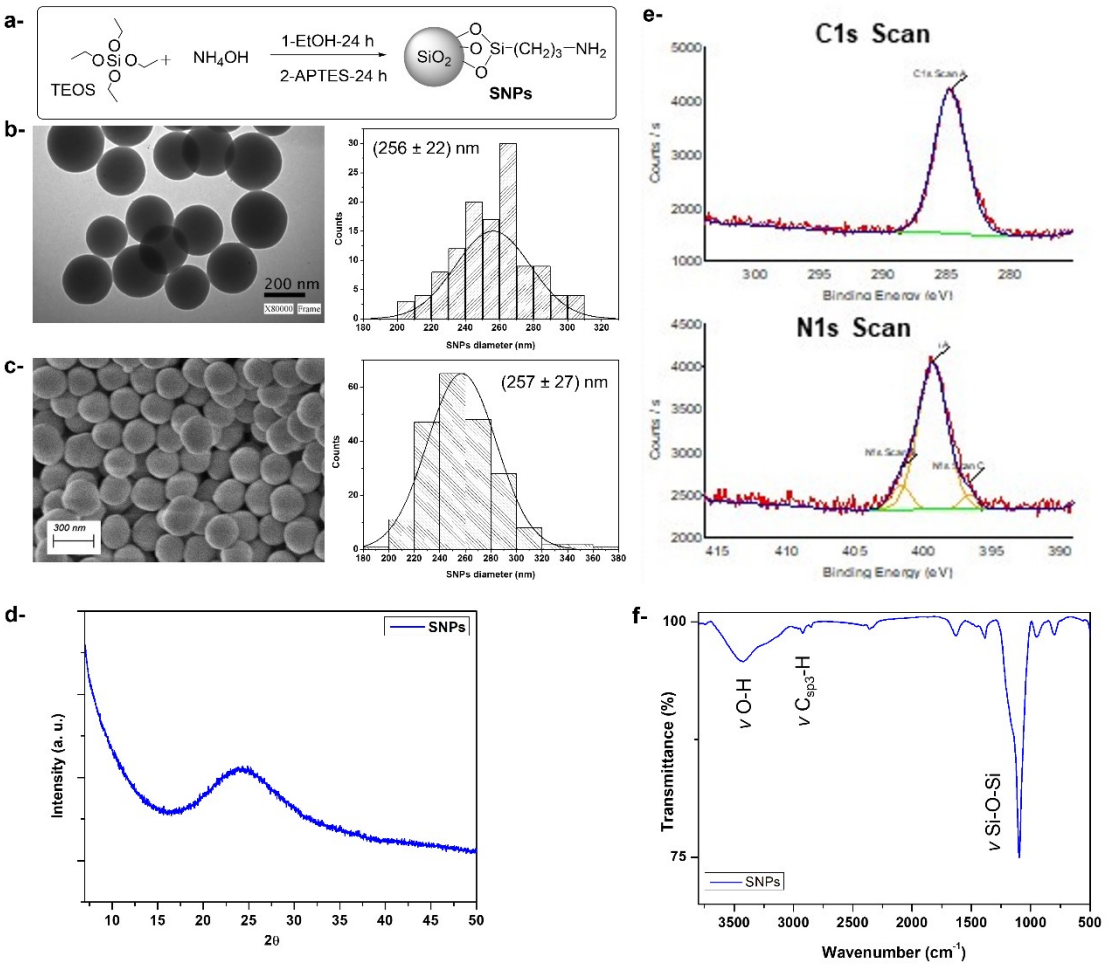

***Figure SI 8**. (a) Synthetic procedure for obtaining functionalized silica nanospheres (SNPs). (b) TEM analysis. (c) SEM analysis. (d) DRX spectrum showing the amorphous structure of SNPs. (e) High-resolution XPS spectra of C1s and N1s of SNPs, demonstrating the presence of APTES. (f) FT-IR spectrum of SNPs showing the vibrations of Si-O-Si and O-H bonds of silica structure and the aliphatic C-H stretching bands corresponding to APTES functionalization.*

9. Methodology approaches for the preparation of supported Pd-NPs onto SNPs and characterization

The synthesis of the supported nanocatalysts was performed following two approaches: (a) sol-immobilization of Pd-PVP or Pd-CMC NPs onto SNPs and (b) in situ (photo)reduction of Pd-NPs in presence of SNPs and stabilizer. Both approaches were performed under batch and continuous flow systems.

Average dimensions and shape of SNPs supported Pd-PVP and Pd-CMC NPs were determined by TEM images. Samples for morphological characterization were prepared by dispersing the solid in a water:iPrOH 1:1 mixture and depositing a drop of the suspension on a 300 mesh formvar-carbon coated copper grid and dried at room temperature. For SEM microscopy and EDS images, the dried samples were deposited in a carbon substrate and covered with Cr.

Size distribution of SNPs and Pd-NPs was established by the average over 100 NPs from different places at each image of all samples. Distribution plots of the size were resolved by fitting data with a Gaussian behavior.

FT-IR spectra were collected preparing the sample on KBr disc.

The XPS spectrum was adjusted to the main spurious C 1s peak at 284.8 eV. To avoid any charging effects during measurement (typically observed in semiconductor-isolated systems), a flood gun to compensate the charge was used. The overcompensation effects by adjusting the spectra during measurement were also tested.

ICP-MS analysis was performed to determine the amount of Pd-NPs on the SNPs silica of each supported catalyst. The aqueous supernatants recovered through centrifugation after the wet impregnation and in situ photoreduction procedures were analyzed. For that, previous digestion of the samples was performed using HNO_3 for 18 h at room temperature. The amount of Pd impregnated on the SNPs was calculated subtracting the moles of Pd remaining in the supernatant, quantified by ICP-MS, from the initial moles of Pd added at the beginning of the supported catalysts procedure. The Pd load in each sample is expressed as mg of Pd per 100 mg of supported catalyst (wt.%), and this value was used to calculate the Pd load in each catalytic reaction.

(a) Sol-immobilization of Pd-PVP or Pd-CMC NPs onto SNPs in batch

In a 250 mL round bottom flask equipped with a magnetic stir bar, 90 mL of water was added and adjusted to pH 1 with H_2SO_4 2 M feedstock solution. Then, 10 mL of colloidal solution of Pd-NPs was added, stirred for 5 min and then 200 mg of SNPs were added. The mixture was stirred overnight at 20°C to obtain Pd-CMC-im-1/SNPs (Table SI 4, entry 1, Figure SI 9) or stirred for 30 min at 20°C or 50°C to obtain Pd-PVP-im/SNPs and Pd-CMC-im-2/SNPs, respectively (Table SI 4, entries 2-3, Figure SI 10). The supported catalyst was recovered through centrifugation for 8 min at 3500 rpm. The supernatant was stored for ICP-MS analysis, and the solid was washed with water. This procedure was repeated two times. Finally, the supported catalyst with a grey color was dried under air at room temperature for 24 h. After this procedure, 120 mg of nanocatalysts were recovered to further be used in catalysis.

Table SI 4. Synthesis of Pd-CMC/SNPs and Pd-PVP/SNPs catalysts. [a]

Entry	Name	Stabilizer	Temp. (°C)	NPs diameter (nm)[d]	Pd loading (wt. %)[e]
1[b]	**Pd-CMC-im-1/SNPs**	**CMC** 0.5 %	20	(6.9 ± 1.1)	0.8
2[c]	**Pd-CMC-im-2/SNPs**		50	(4.5 ± 1.0)	1.0
3[c]	**Pd-PVP-im/SNPs**	**PVP** 2.0 %	20	(3.0 ± 0.8)	3.4

a- Sol-immobilization conditions: 5 mL of colloidal Pd NPs solution, 100 mg of SNPs, water adjusted to pH 1 with H_2SO_4, stirring. b- Stirred overnight. c- Stirred 30min. d- Determined by TEM analysis. e- Determined by ICP-MS analysis.

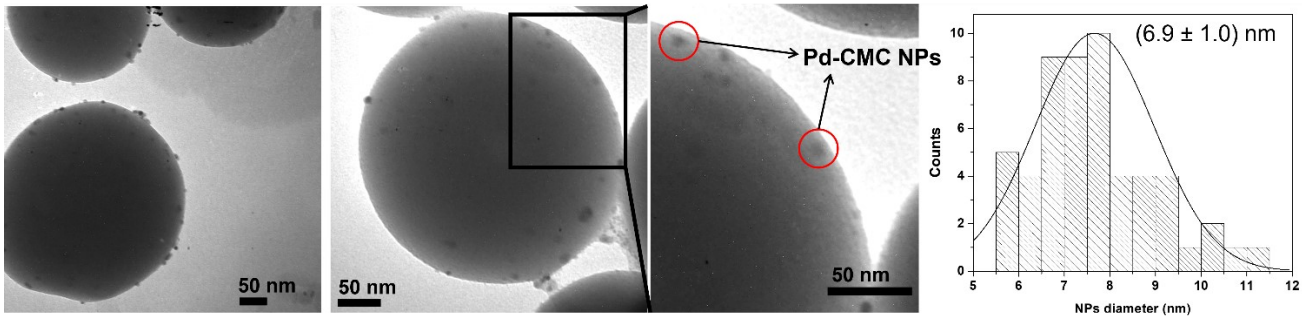

***Figure SI 9**. TEM micrographs and histogram of immobilized Pd-NPs stabilized with 0.5% w/v of CMC onto SNPs. The Pd load was 0.8 wt.%, which represented 80% of the initial mass of Pd.*

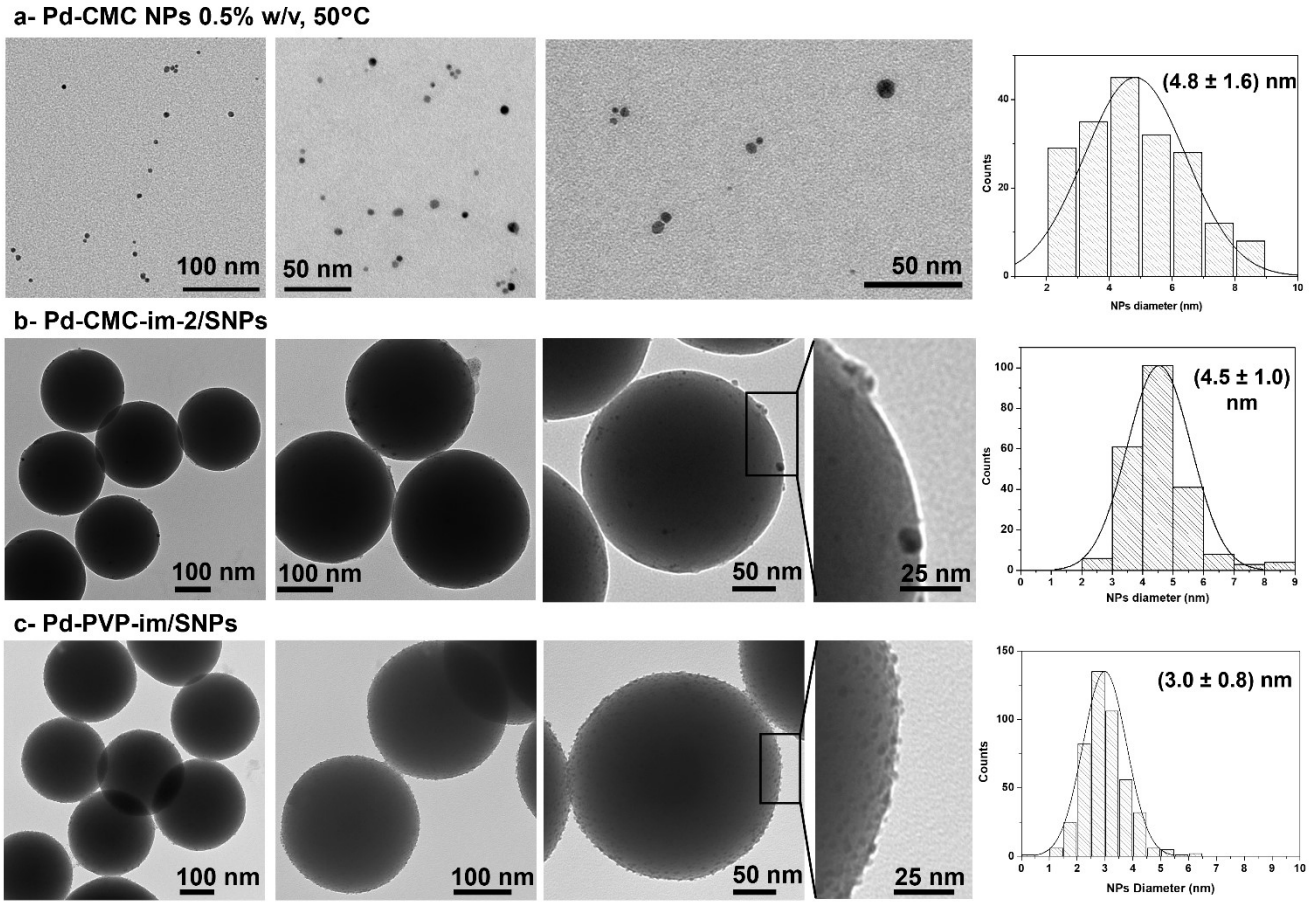

Figure SI 10. *TEM micrographs and histograms of Pd-NPs synthetized using (a) CMC 0.5% w/v at 50°C, then (b) immobilized onto SNPS at 50°C, and (c) Pd-PVP NPs 2.0% w/v immobilized at 20°C onto SNPs.*

(b) Synthesis *in situ* of Pd-NPs in presence of SNPs in batch

In a 10 mL scintillation vial equipped with a magnetic stir bar, 5 mL of a mixture of stabilizer (PVP or CMC), reducing agent (citrate and/or oxalate salts) and H_2PdCl_4 2 mM was prepared following the same protocol for the synthesis of colloidal Pd NPs (see section 3). Then, 10.1 mg of SNPs were added, the vial was sealed and Ar bubbled for 5 min to saturate the solution. Next, the mixture was irradiated in the photochemical reactor under vigorous magnetic stirring until it changed color to brown. Finally, the vial was opened, and the supported catalyst was recovered through centrifugation as described in the previous section (see section 9.a).

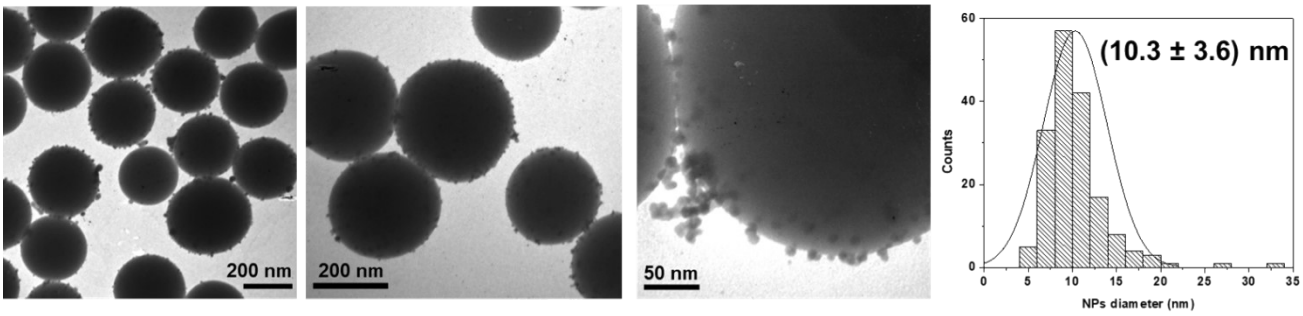

***Figure SI 11**. In situ (photo)reduction of Pd^{2+} salts onto SNPs in absence of stabilizers.*

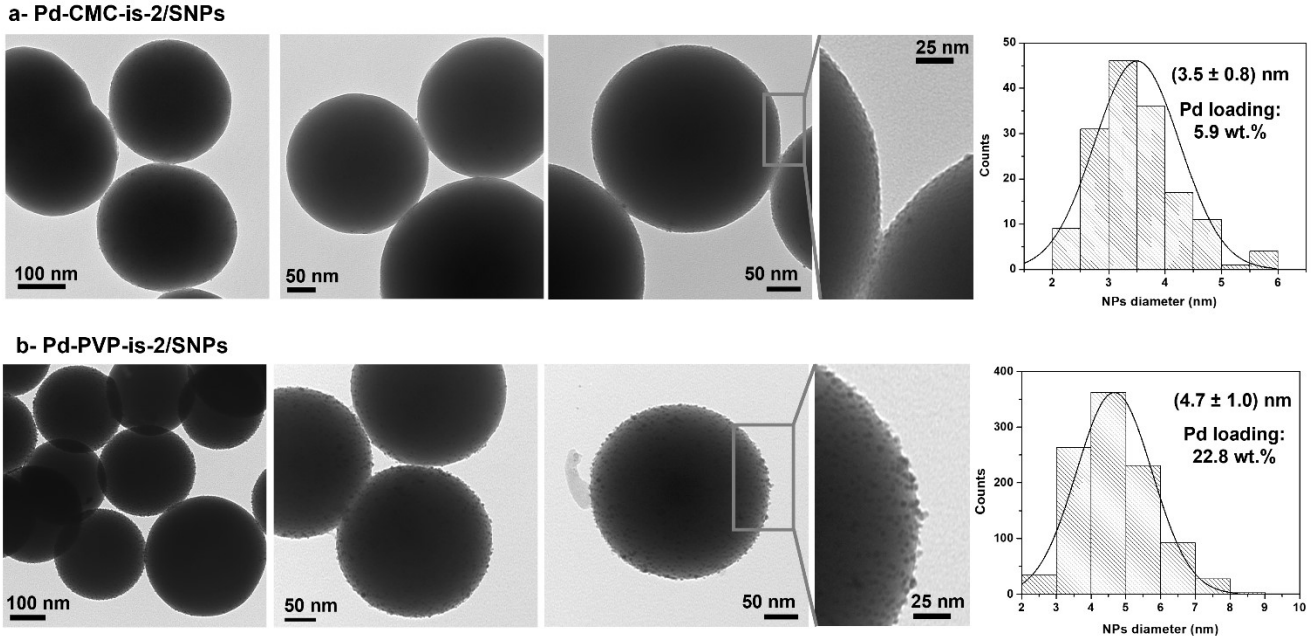

***Figure SI 12**. TEM analysis of Pd-NPs synthetized by in situ (photo)reduction using (a) CMC and (b) PVP as stabilizers, and with an initial Pd^{2+}/SNPs mass ratio of 0.6.*

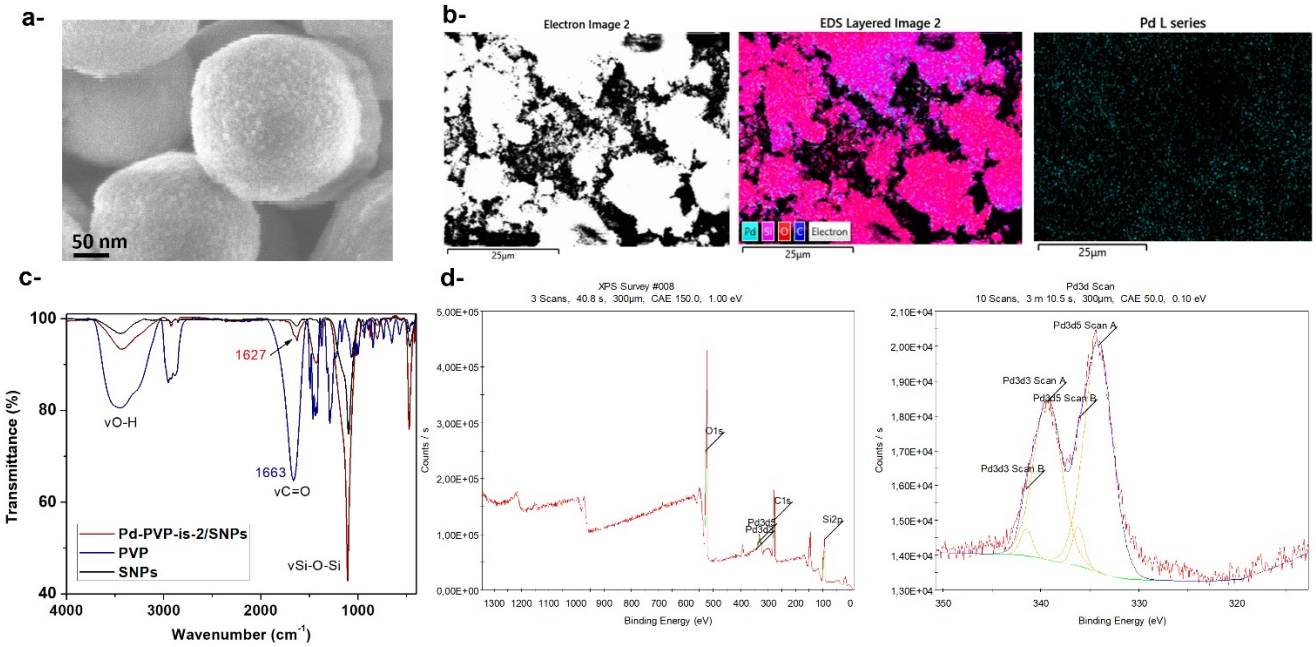

***Figure SI 13**. Characterization of **Pd-PVP-is-2/SNPs**. (a) SEM micrograph. (b) EDS map spectrum and Pd homogeneously distributed along the sample. (c) FT-IR spectra of the sample, PVP and SNPs. (d) XPS survey and Pd3d high-resolution XPS spectrum.*

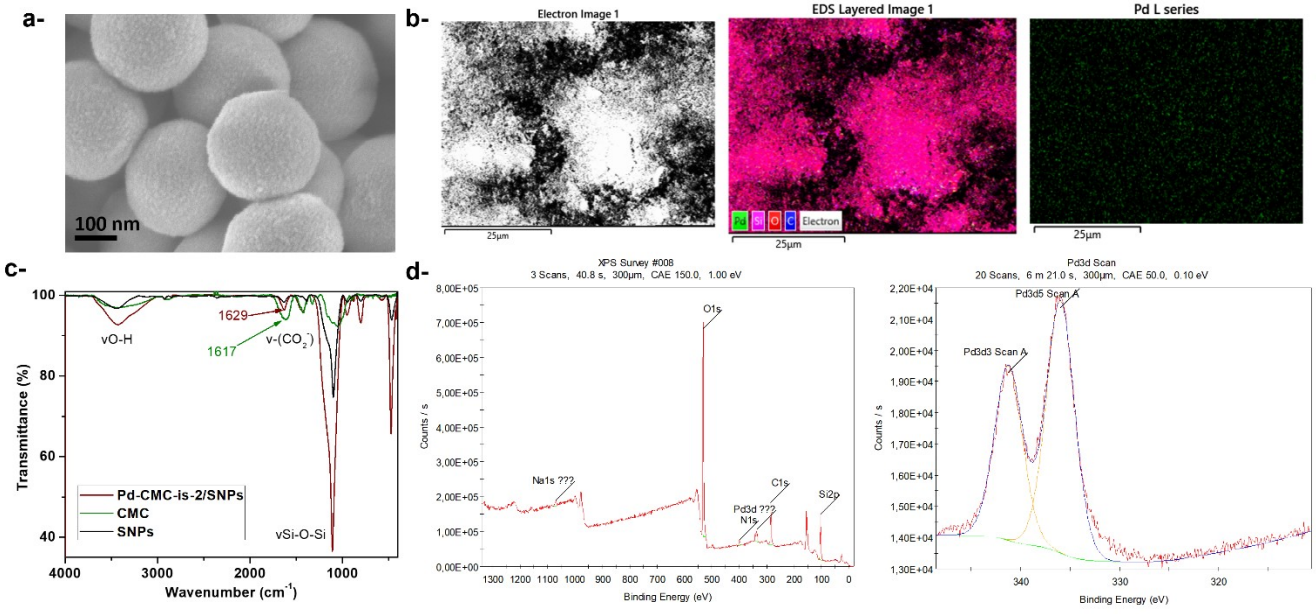

***Figure SI 14**. Characterization of **Pd-CMC-is-2/SNPs**. (a) SEM micrograph. (b) EDS map spectrum and Pd homogeneously distributed along the sample. (c) FT-IR spectra of the sample, CMC and SNPs. (d) XPS survey and Pd3d high-resolution XPS spectrum.*

(c) Sol-immobilization of Pd-PVP or Pd-CMC NPs onto SNPs in continuous flow system

A colloidal solution of Pd-PVP (2.0% w/v) or Pd-CMC (0.5% w/v) NPs (48 mL, 2 mM) was charged into a plastic syringe. On the other hand, 30 mg of SNPs were suspended in 48 mL water, adjusted to pH=1 with H_2SO_4 2 M and loaded into a second plastic syringe with a stir bar inside. The syringe pump together with a portable magnetic stirrer bar were placed in vertical position in order to keep the SNPs suspension as much homogenous as possible and to avoid clogging. Both syringes were connected through a mesoscale photochemical flow reactor (6.56 mL with 0.75 mm ID FEP-tubing) and the mixture was continuously pumped into the reactor by using the syringe pump (0.109 mL/min) at room temperature. Finally, the heterogeneous material was collected and the supported catalyst was recovered through centrifugation for 8 min at 3500 rpm. The supernatant was stored for ICP-MS analysis, and the solid was washed with water. This procedure was repeated two times. Finally, the supported catalyst with a grey color was dried under air at room temperature for 24 h.

(d) Synthesis *in situ* of Pd-PVP NPs in presence of SNPs in continuous flow system

A mixture of solution of PVP (2.0% w/v), sodium citrate and sodium oxalate salts (molar ratio Pd^{2+}/reducing agent 1:10) and 48 mL of feedstock aqueous solution of H_2PdCl_4 4 mM, was saturated by Ar and charged into a syringe. On the other hand, 30 mg of SNPs were suspended in 48 mL water, adjusted to pH=1 with H_2SO_4 2 M saturated by Ar and charged into a second plastic syringe with a stir bar inside. The syringe pump together with a portable magnetic stirrer bar were placed in vertical position in order to keep the SNPs suspension as much homogenous as possible and to avoid clogging. Both syringes were connected through a mesoscale photochemical flow reactor (6.56 mL with 0.75 mm ID FEP-tubing) and the mixture was continuously pumped and irradiated for 30 min through a blue-LED reactor (15 x 5 W at 462 nm). Finally, the heterogeneous material was collected in an open glass vial to ensure that the

reaction stops. The supported catalyst was recovered through centrifugation for 8 min at 3500 rpm. The supernatant was stored for ICP-MS analysis, and the solid was washed with water. This procedure was repeated two times. Finally, the supported catalyst with a grey color was dried under air at room temperature for 24 h.

10. Representative procedure for the Suzuki-Miyaura cross-coupling reaction catalyzed by supported Pd nanocatalysts

Into a 10 mL tube reaction with a Teflon screw-cap septum equipped with a magnetic stirrer, *p*-bromoacetophenone (**1**) (0.12 mmol), arylboronic acid (**2**) (0.18 mmol) and K_3PO_4 (0.37 mmol), and 1.0 mg of the supported Pd-NPs catalyst was added. Then, EtOH (0.7 mL) and water (2.0 mL) were added. The reaction mixture was heated at 60°C in an oil bath for 2 h. After being cooled to room temperature, the mixture was opened to the air, diluted with water, and centrifugated at 3500 rpm for 8 min. Then, 0.05 mmol of benzophenone was added to the mixture of organic phase and aqueous supernatant, and it was extracted using 2 x 5 mL of ethyl acetate. The organic phase was dried with anhydrous Na_2SO_4 and analysed by gas chromatography. The biaryl product was purified by silica-gel column chromatography.

The moles of Pd in each reaction to calculate the TOF values were obtained from the Pd loading of each catalyst determined by ICP-MS analysis.

11. Representative procedure for the Suzuki-Miyaura cross-coupling with different aryl halides and phenylboronic acids

To explore the scope of the reaction, the procedure described in Section 10 was performed using different substrates and aryl boronic acids. The amount of Pd-CMC-is-1/SNPs catalyst, temperature and reaction time were optimized. The reactions were quantified by GC using

benzophenone as internal standard. Products were purified and then characterized through GCMS and NMR using $CDCl_3$ as solvent.

The scope of the Pd-CMC-is-1/SNPs catalyst is shown in Table SI 5 below.

Table SI 5. Scope of Suzuki-Miyaura cross-coupling reaction between aryl halides and phenylboronic acids under mild reaction conditions using Pd-CMC-is-1/SNPs

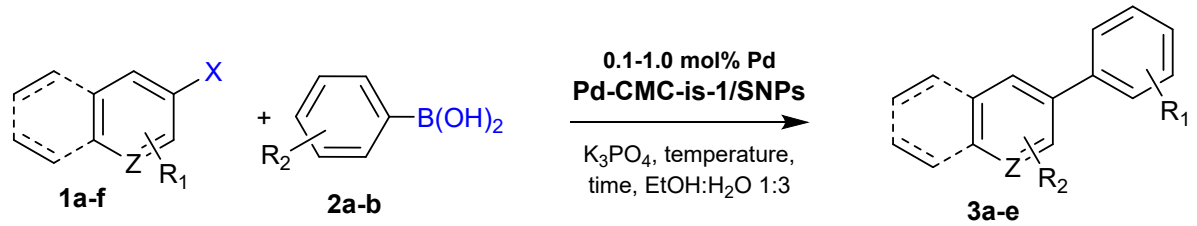

Z= C, N
X= I, Br
R_1= OMe, CN, COMe

2a R_2= H
2b R_2= F

Entry	Substrate	Aryl boronic acid	Product		Pd loading (mol%)	T (°C)	Time (h)	Yield (%)
1	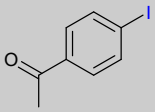	**2a**	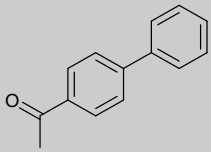	**3a**	0.18	60	1	**97**
2	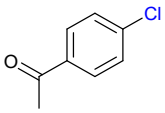	**2a**	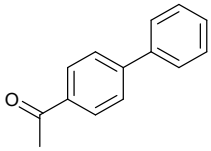	**3a**	1.0	98	24	**5**
3	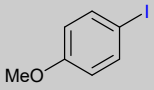	**2b**	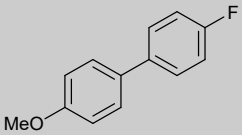	**3b**	0.14	60	2	**90**
4	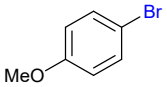	**2b**	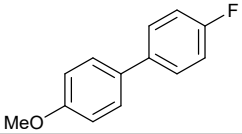	**3b**	0.14	80	20	**100**
5	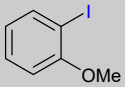	**2a**	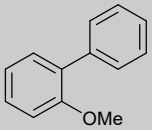	**3c**	0.14	80	2	**92**
6	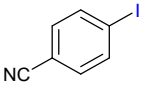	**2a**	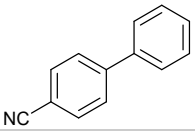	**3d**	0.47	80	2	**89**
7	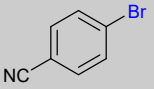	**2a**	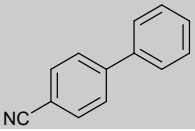	**3d**	0.47	80	2	**92**

8	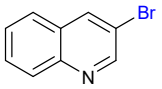	**2a**	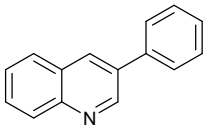	**3e**	1.0	98	24	**48**

Reaction conditions: 0.12 mmol of **1**, 0.18 mmol **2**, 0.37 mmol K_3PO_4, 1-8 Pd-CMC-is-1/SNPs nanocatalyst, ethanol:water 1:3

12. Representative procedure for recycling experiment with supported Pd-NPs on SNPs

The recycle of the supported Pd-NPs catalysts was performed after carried out the reaction following the procedure previously described in Section 10, and using 12.5 mg of the supported Pd-NPs catalysts. After the reaction time finished, the reaction tube was cooled to room temperature and 2 mL of ethyl acetate was added. The reaction crude was mixed and let it rest until the aqueous and organic layers separated. Then, the organic phase was removed, and the aqueous phase was centrifugated for 8 minutes at 3500 rpm. After that, the supernatant was removed and mixed with the organic phase, and the pellet was washed two more times with water. Then, 0.05 mmol of benzophenone was added to the mixture of organic phase and aqueous supernatant, and it was extracted using 2 x 5 mL of ethyl acetate. The organic phase was dried with anhydrous Na_2SO_4 and analysed by gas chromatography.

The grey solid recovered after the centrifugation cycles was used for the next reaction cycle, adding a new batch of 4-bromoacetophenone (**1a**) (0.12 mmol), phenylboronic acid (**2a**) (0.18 mmol) and K_3PO_4 (0.37 mmol), EtOH (0.7 mL) and water (2.0 mL). This whole procedure was repeated after each cycle.

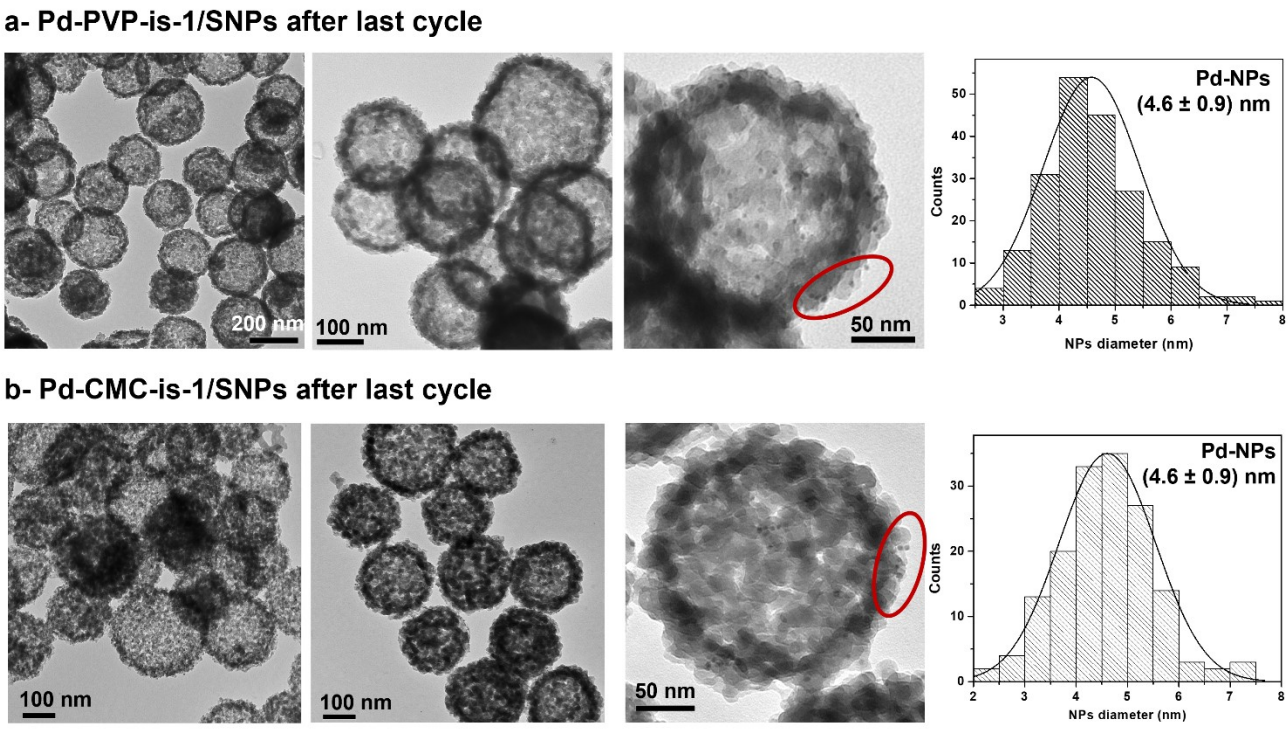

Figure SI 15. TEM micrographs and Pd-NPs diameters of (a) Pd-PVP-is-1/SNPs and (b) Pd-CMC-is-1/SNPs catalysts after the recycling experiment. Red circles indicate the Pd-NPs immobilized on the SNPs matrix

13. Characterization data of Suzuki-Miyaura cross-coupling reaction products

All products were purified and analyzed through NMR and GCMS. All data was in good agreement with the previous reported in literature.

- **1-([1,1'-biphenyl]-4-yl)ethan-1-one (3a)[11]**

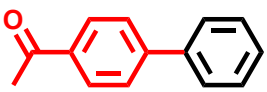

The product was purified through silica gel chromatography using pentane/diethyl ether (80:20) and was obtained as a white solid.

1H RMN (400 MHz; $CDCl_3$) δ: 8,05-8,02 (m; 2H); 7,71-7,67 (m; 2H); 7,63 (dt; J = 8,3; 1,8 Hz; 2H); 7,49-7,45 (m; 2H); 7,43-7,38 (m; 1H); 2,64 (s; 3H).

13C RMN (101 MHz; $CDCl_3$) δ: 197,8 (C); 145,9 (C); 140,0 (C); 136,0 (C); 129,1(CH); 129,0 (CH); 128,4 (CH); 127,4 (CH); 127,3 (CH); 26,8 (CH_3).

GCMS (70eV): 196 (52, M+), 181 (100), 152 (69), 76 (47), 63 (15), 51 (13)

- **1-(4'-fluoro-[1,1'-biphenyl]-4-yl)ethan-1-one (3b)[12]**

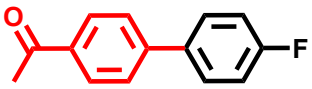

The product was purified through silica gel chromatography using hexane/ethyl acetate (80:20) and was obtained as a white solid.

1H: δ ^{1}H NMR (400 MHz, CDCl3) δ 8.03 (d, *J* = 8.4 Hz, 2H), 7.64 (d, *J* = 8.6 Hz, 2H), 7.59 (dd, *J* = 8.9, 5.3 Hz, 2H), 7.16 (t, *J* = 8.7 Hz, 2H), 2.64 (s, 3H).

13C: ^{13}C NMR (101 MHz, $CDCl_3$) δ 197.52, 163.02 (d, *J* = 248.1 Hz), 144.74, 136.05 (d, *J* = 3.3 Hz), 135.93 (d, *J* = 4.2 Hz), 128.95, 128.87, 127.06, 115.91 (d, *J* = 23.6 Hz), 26.61.

19F: ^{19}F NMR (376 MHz, $CDCl_3$) δ -114.14.

GCMS (70eV): 214 (46, M+), 200 (15), 199 (100), 171 (47), 170 (60), 85 (17)

- **2-methoxy-1,1'-biphenyl (3c)[13]**

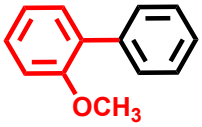

The product was purified through silica gel chromatography using hexane/ethyl acetate (80:20) was obtained as yellowish oil.

^{1}H NMR (400 MHz, $CDCl_3$) δ 7.62 (ddt, *J* = 7.5, 2.4, 1.1 Hz, 2H), 7.53 – 7.45 (m, 2H), 7.45 – 7.36 (m, 3H), 7.15 – 7.02 (m, 2H), 3.87 (s, 3H).

^{13}C NMR (101 MHz, $CDCl_3$) δ 156.58, 138.66, 130.99, 130.83, 129.66, 128.72, 128.08, 127.01, 120.94, 111.35, 77.48, 77.16, 76.84, 55.62.

CG-MS (70eV) *m/z* (%): 63 (21); 91 (20); 115 (47); 141 (51); 169 (56); 183 (21); [*M*+] 184 (100); [*M*++*1*] 185 (14).

- **[1,1'-biphenyl]-4-carbonitrile (3d)[11]**

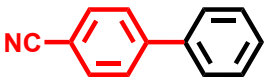

The product was purified through silica gel chromatography using pentane/diethyl ether (90:10) and was obtained as a white solid.

^{1}H RMN (400 MHz; $CDCl_3$) δ: 7.74-7.67 (m, 1H), 7.61-7.58 (m, 1H), 7.51-7.41 (m, 1H).

^{13}C RMN (101 MHz; $CDCl_3$) δ: 145.8,139.3, 132.7, 129.2, 128.8, 127.8, 127.3, 119.0, 111.0.

CG-MS (70eV) *m/z* (%): 76 (14); 151 (15); 178 (25); [*M*+] 179 (100); [*M*++*1*] 180 (14).

- **3-phenylquinoline (3e)[14]**

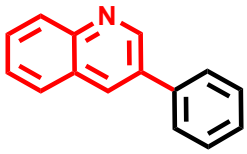

The product was purified through silica gel chromatography using hexane/dichloro methane/ethyl acetate (50:45:5) and was obtained as a white solid.

^{1}H NMR (400 MHz, $CDCl_3$) δ 9.20 (d, *J* = 2.3 Hz, 1H), 8.31 (d, *J* = 1.3 Hz, 1H), 8.15 (d, *J* = 8.4 Hz, 1H), 7.89 (dd, *J* = 8.2, 1.5 Hz, 1H), 7.78 – 7.69 (m, 3H), 7.59 (ddd, *J* = 8.1, 6.9, 1.2 Hz, 1H), 7.56 – 7.51 (m, 2H), 7.48 – 7.42 (m, 1H).

^{13}C NMR (101 MHz, $CDCl_3$) δ 150.12, 147.53, 138.07, 134.02, 133.39, 129.54, 129.42, 129.34, 128.27, 128.19, 128.16, 127.60, 127.16.

CG-MS (70eV) *m/z* (%): 76 (32); 88 (27); 89 (23); 102 (18); 176 (13); 204 (51); [*M*+] 205 (100); [*M*++*1*] 206 (16).

14. NMR spectra of Suzuki-Miyaura cross-coupling reaction products

- **1-([1,1'-biphenyl]-4-yl)ethan-1-one (3a)**

^{1}H NMR (400 MHz, $CDCl_3$)

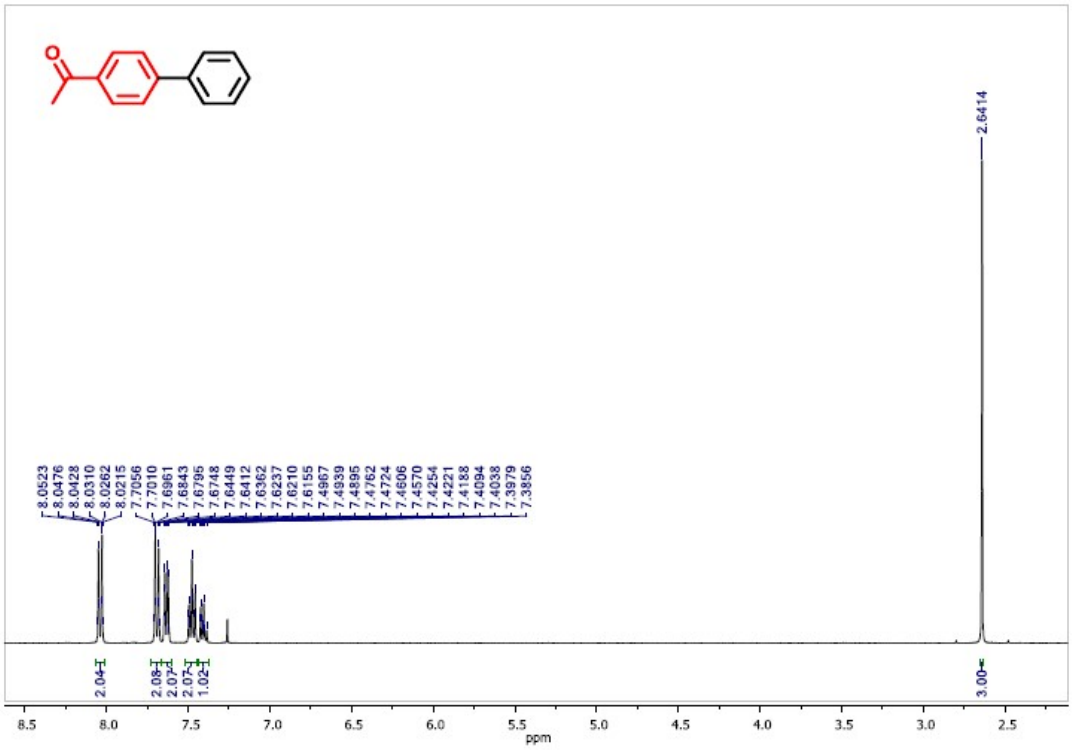

^{1}H NMR (400 MHz, $CDCl_3$)

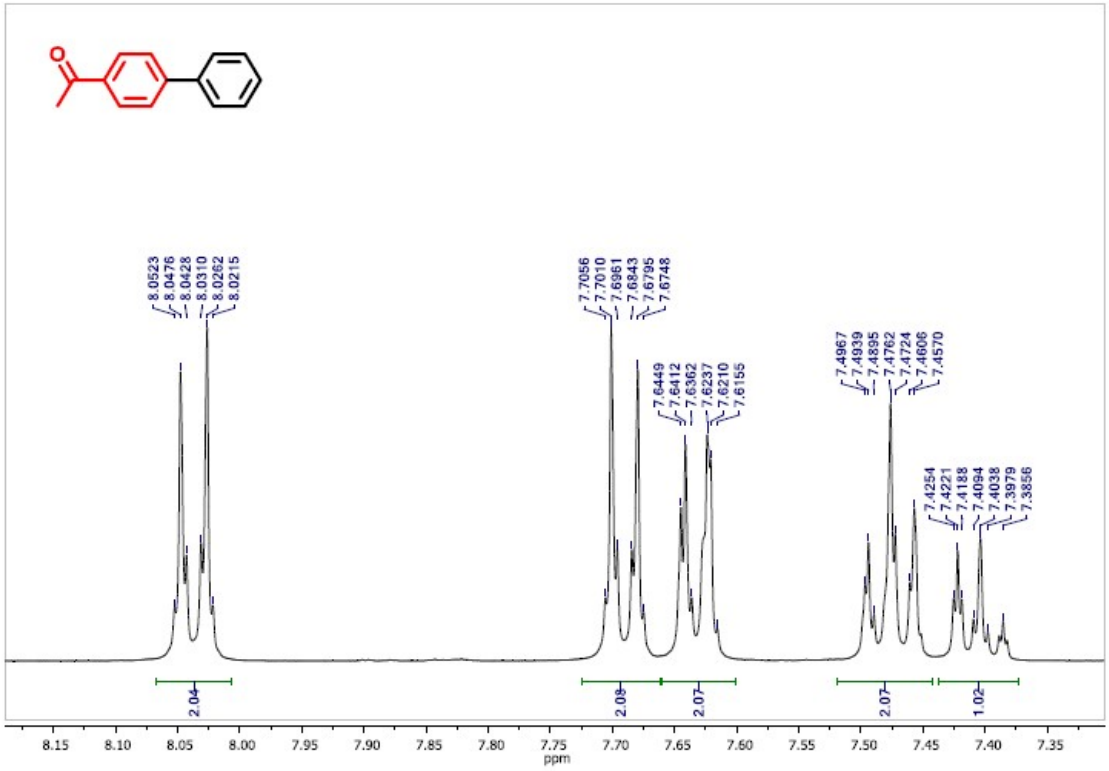

^{13}C NMR (101 MHz, $CDCl_3$)

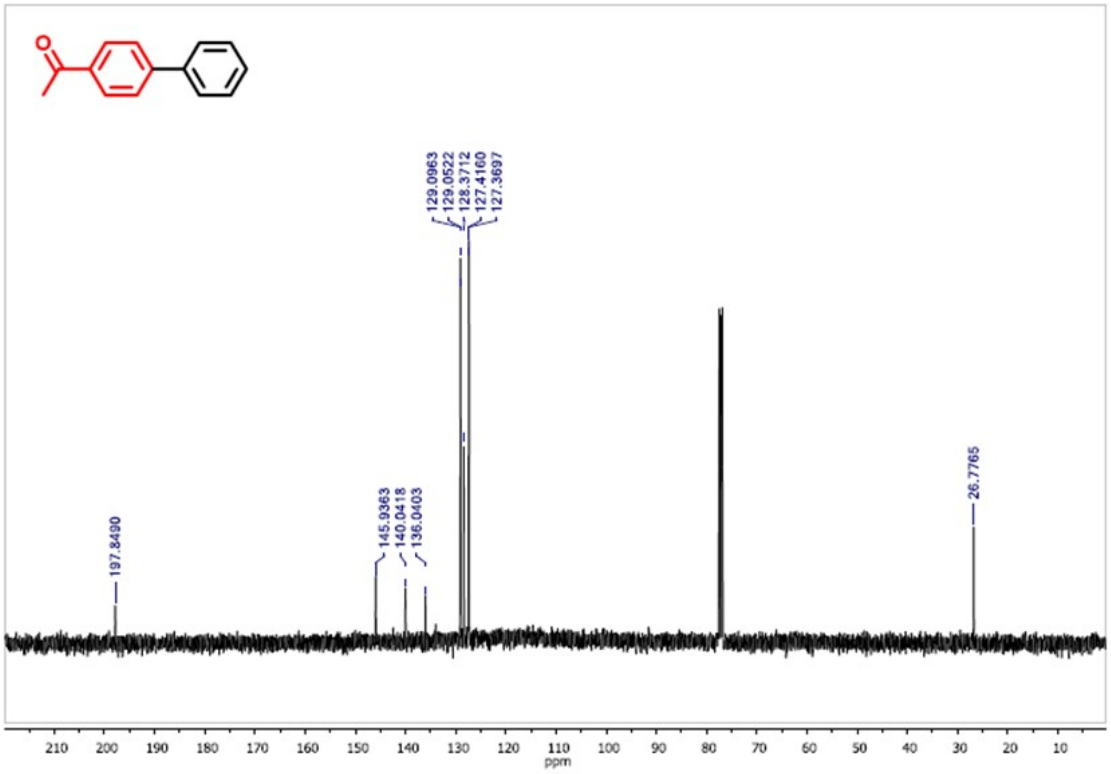

- **1-(4'-fluoro-[1,1'-biphenyl]-4-yl)ethan-1-one (3b)**

^{1}H NMR (400 MHz, $CDCl_3$)

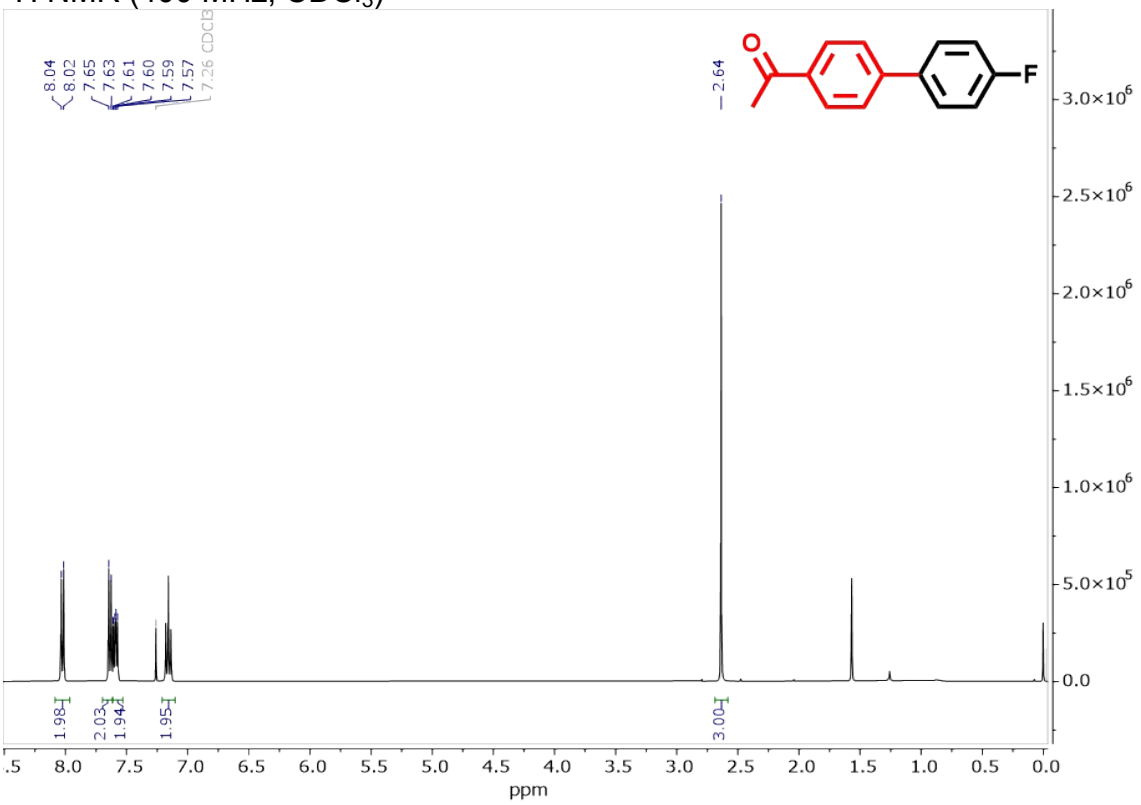

^{1}H NMR (400 MHz, $CDCl_3$)

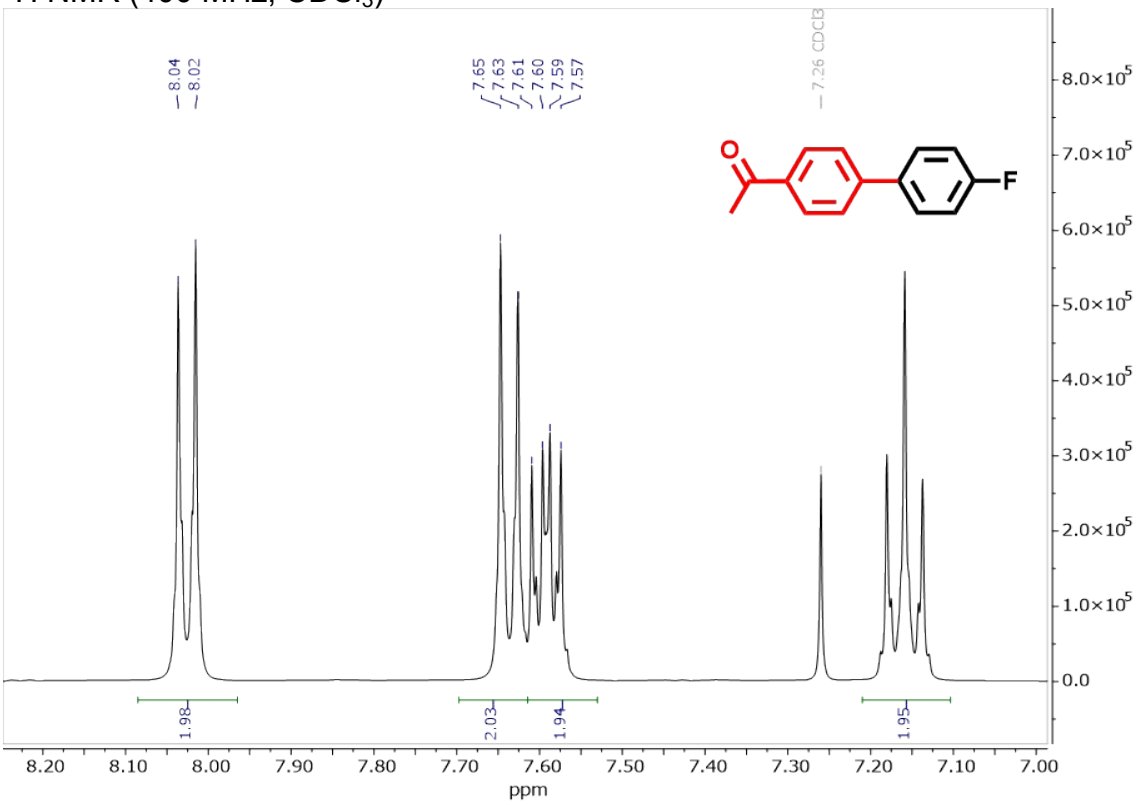

^{13}C NMR (101 MHz, $CDCl_3$)

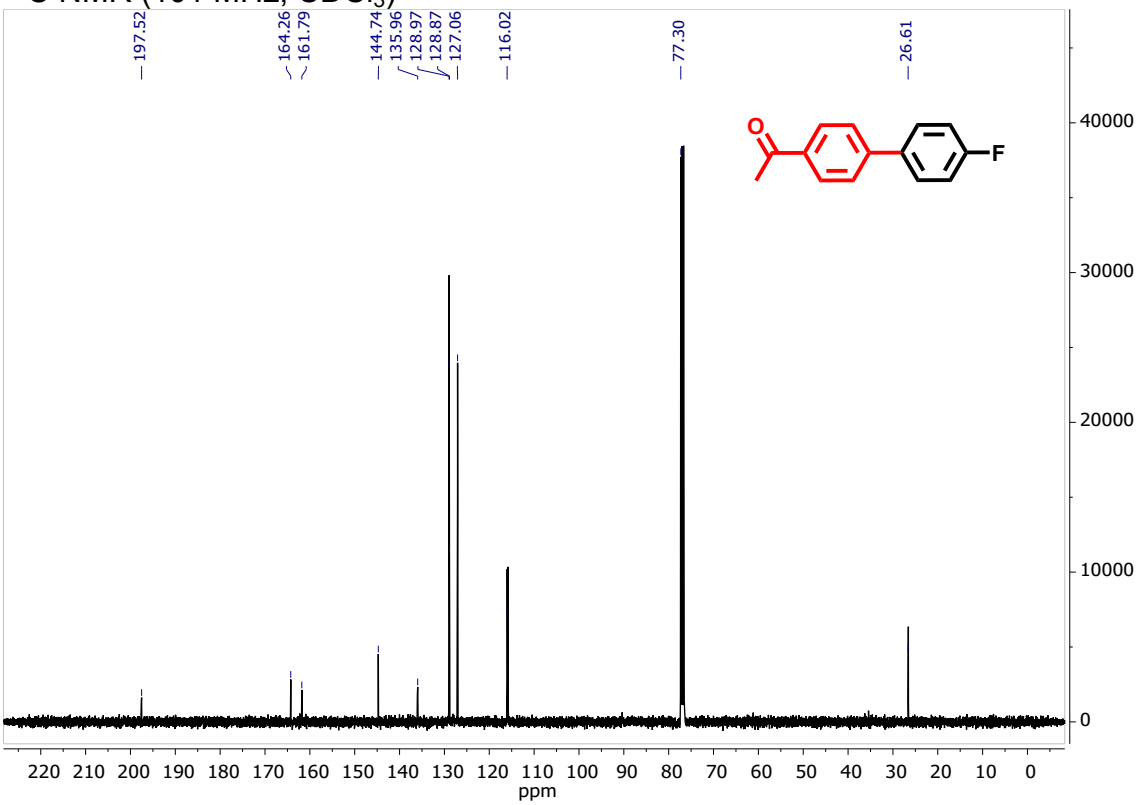

^{19}F NMR (376 MHz, $CDCl_3$)

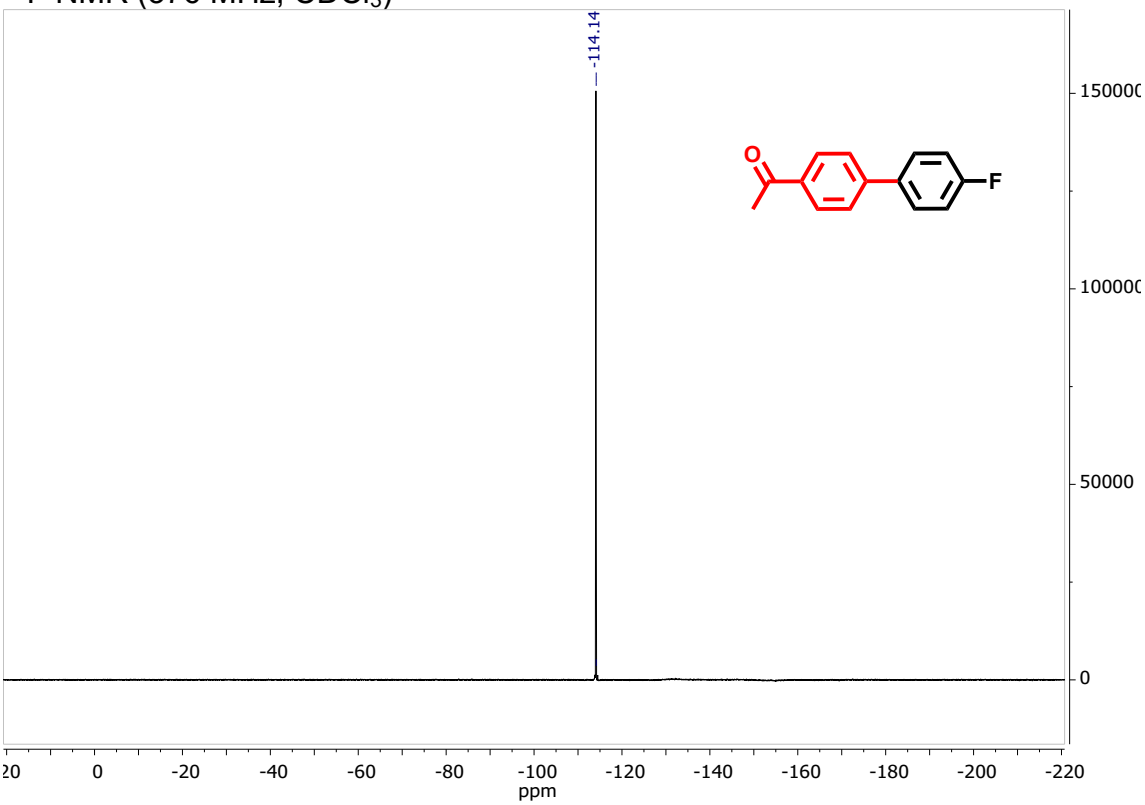

- **2-methoxy-1,1'-biphenyl (3c)**

^{1}H NMR (400 MHz, $CDCl_3$)

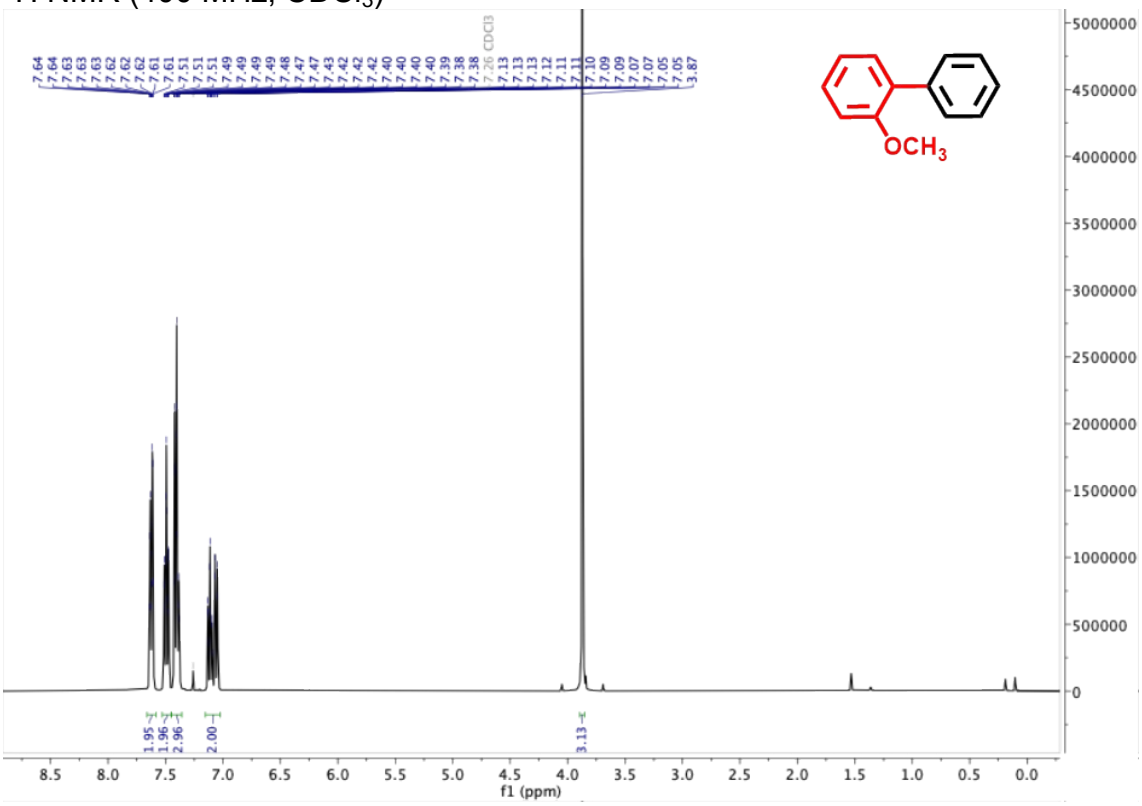

^{1}H NMR (400 MHz, $CDCl_3$)

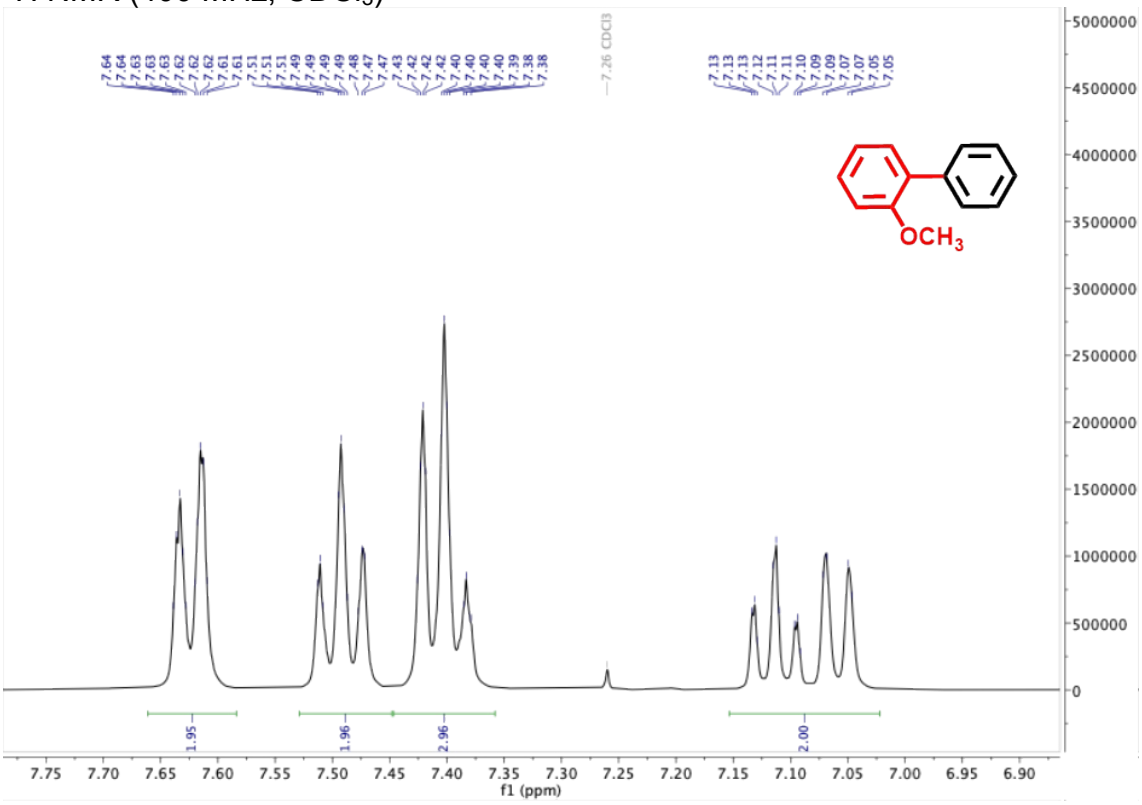

^{13}C NMR (101 MHz, $CDCl_3$)

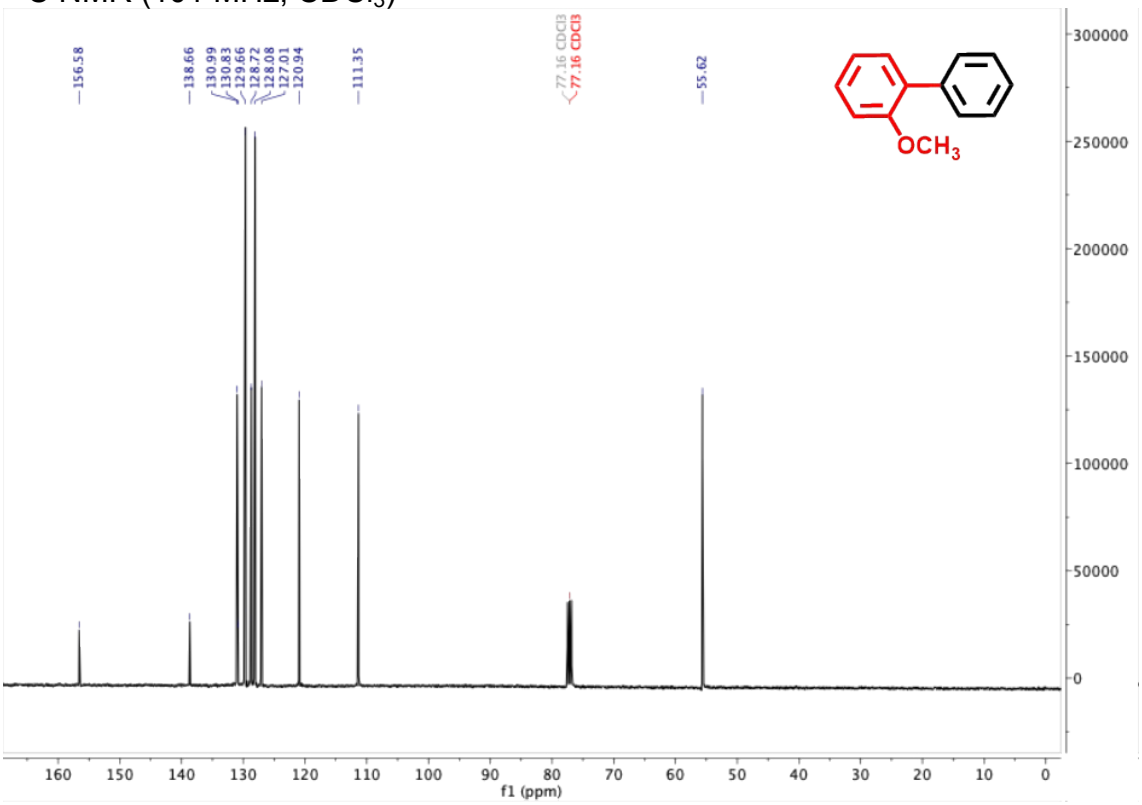

- **[1,1'-biphenyl]-4-carbonitrile (3d)**

^{1}H NMR (400 MHz, $CDCl_3$)

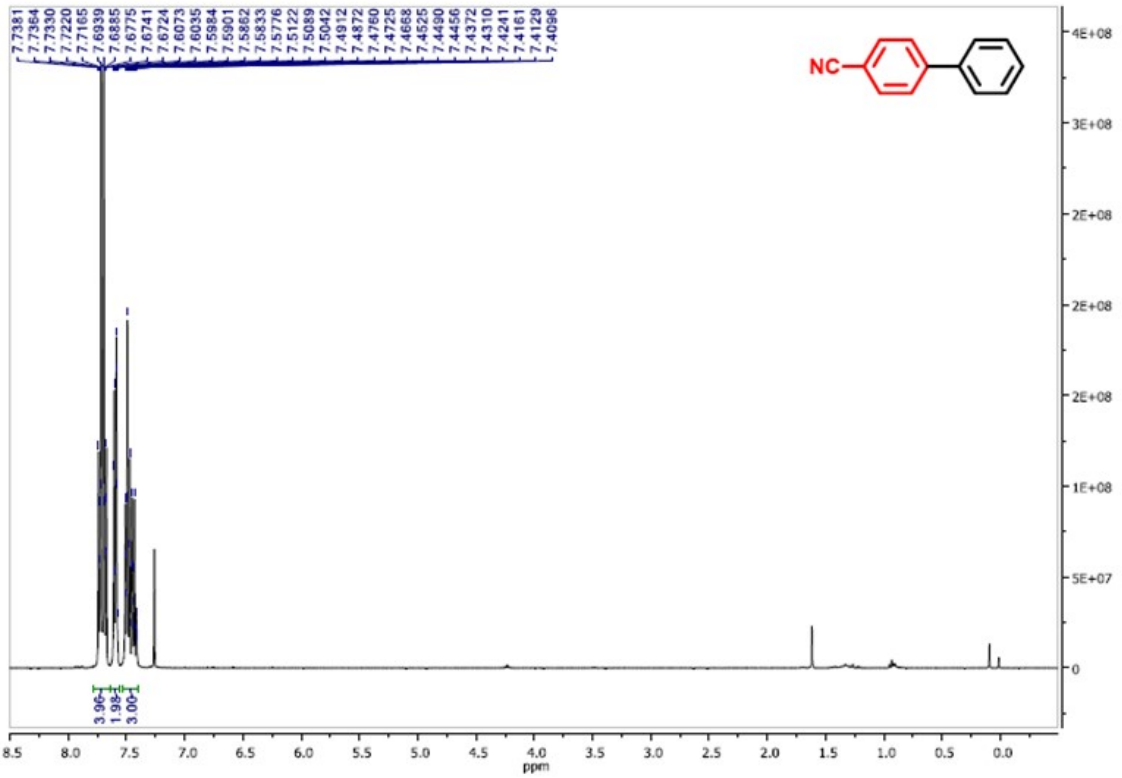

^{1}H NMR (400 MHz, $CDCl_3$)

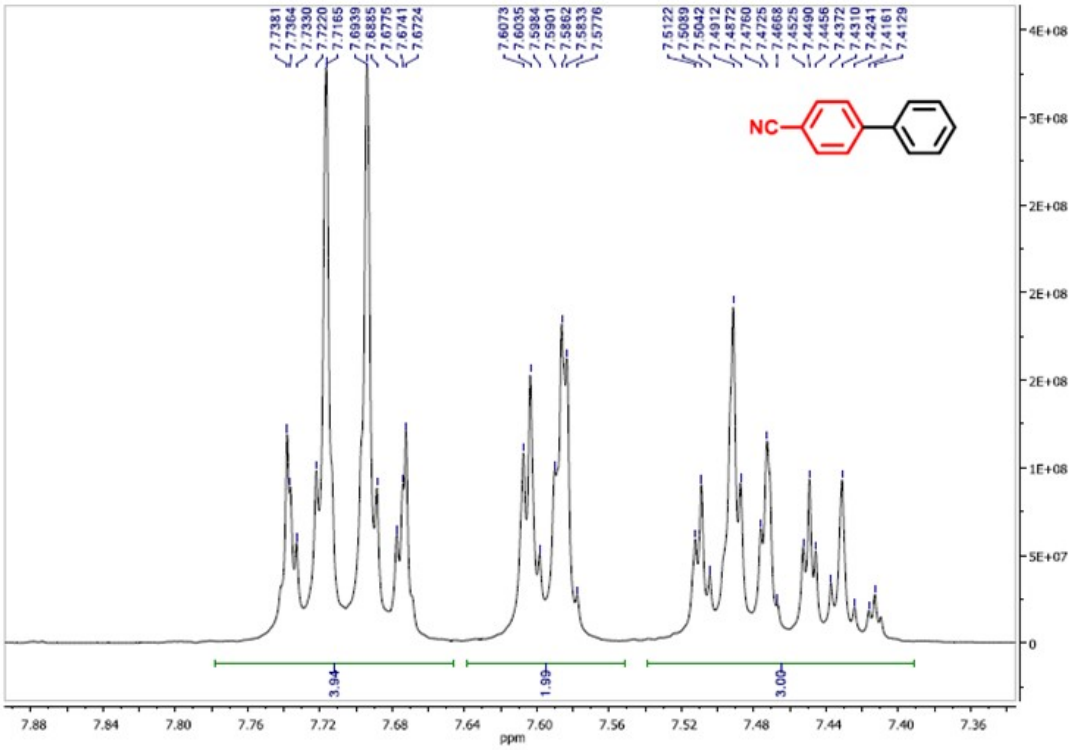

^{13}C NMR (101 MHz, $CDCl_3$)

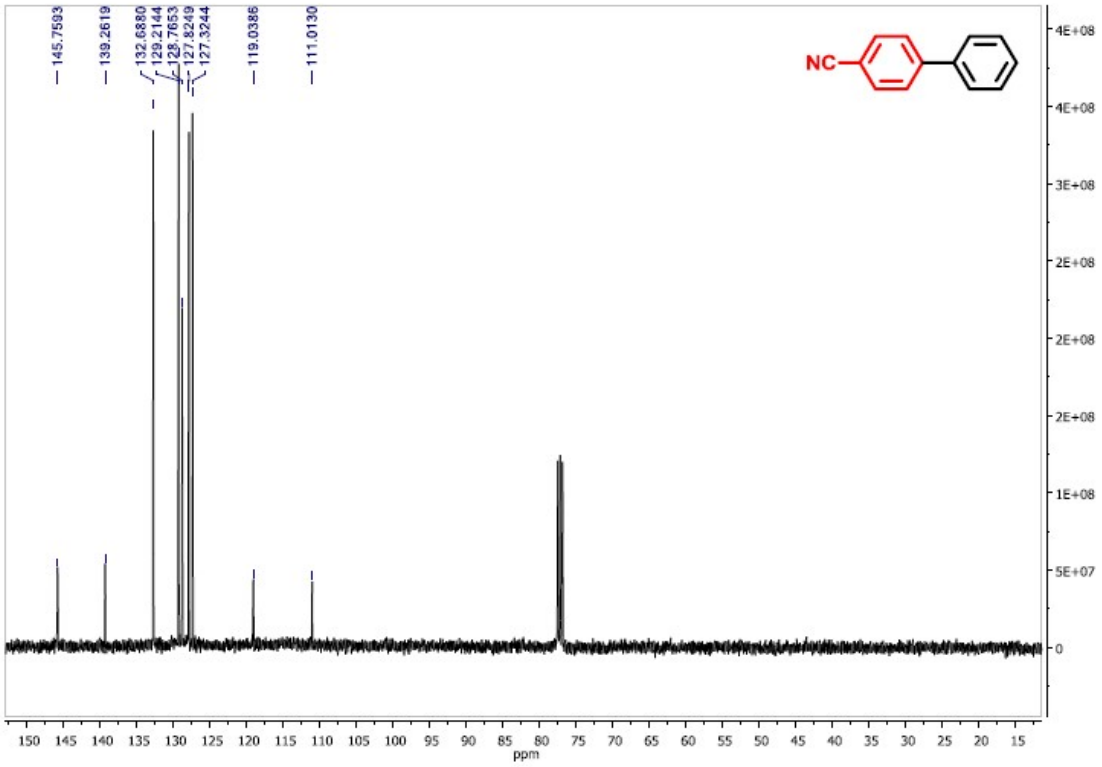

- **3-phenylquinoline (3e)**

^{1}H NMR (400 MHz, $CDCl_3$)

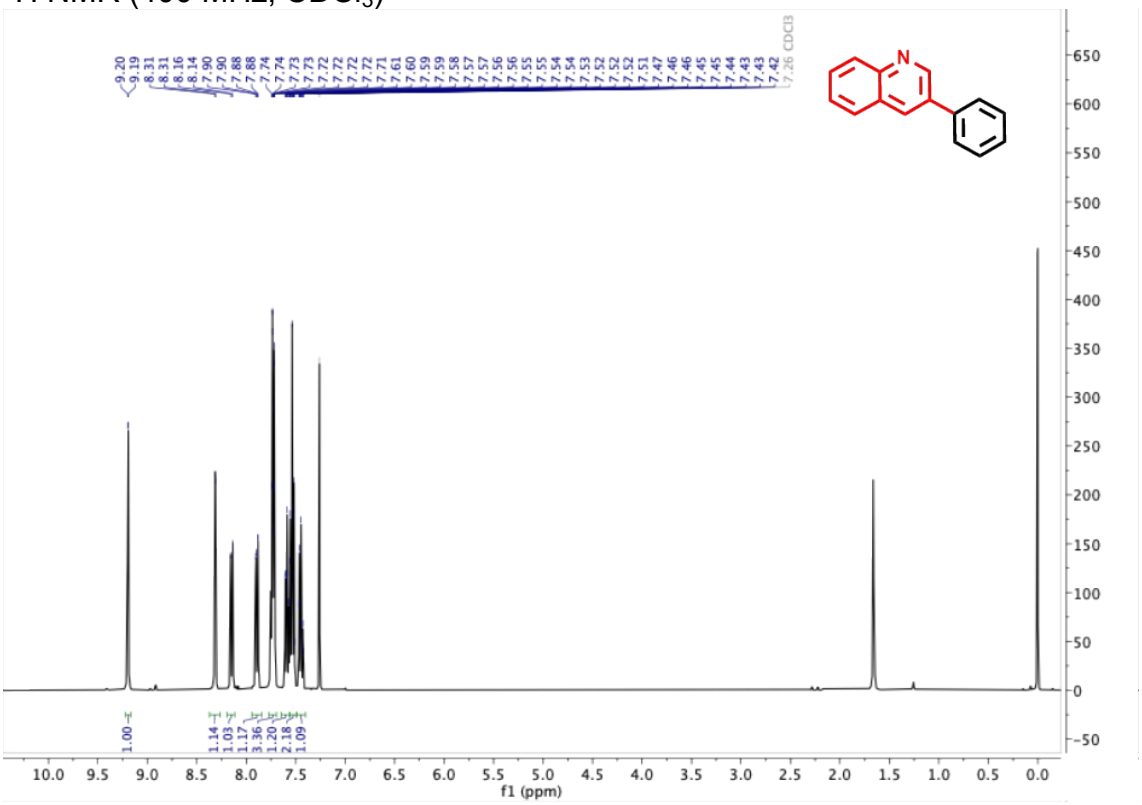

^{1}H NMR (400 MHz, $CDCl_3$)

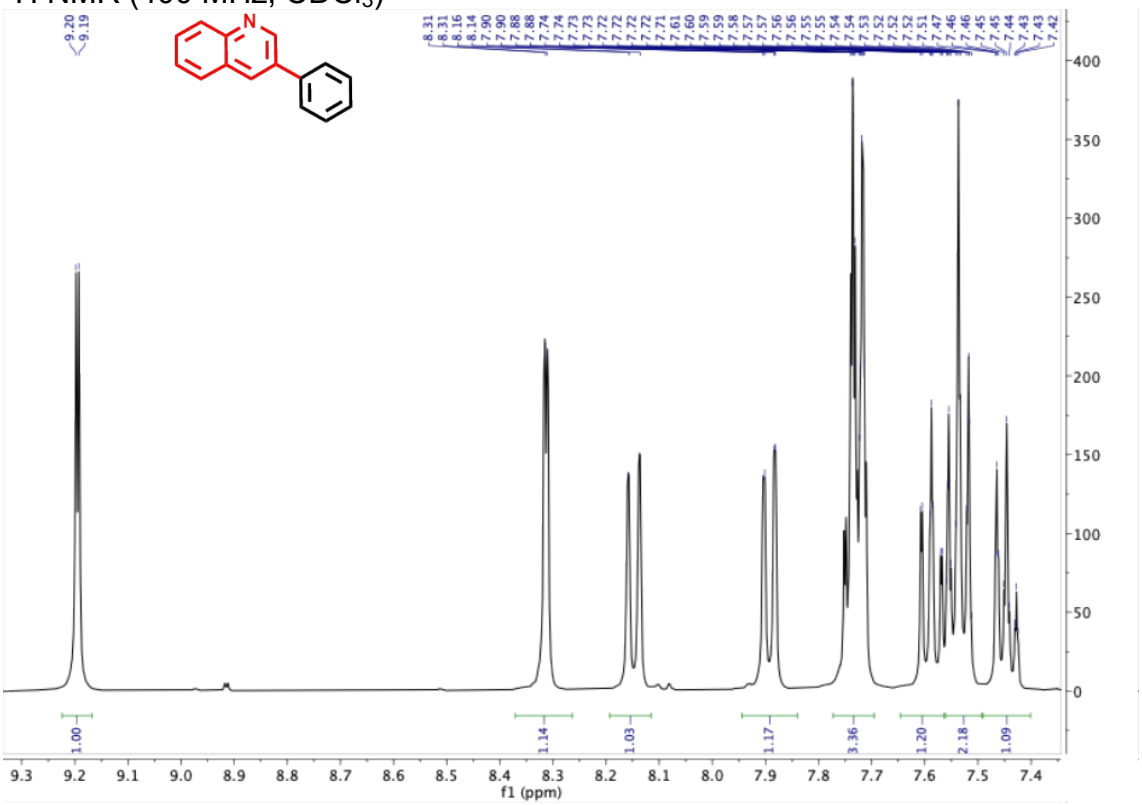

^{13}C NMR (101 MHz, $CDCl_3$)

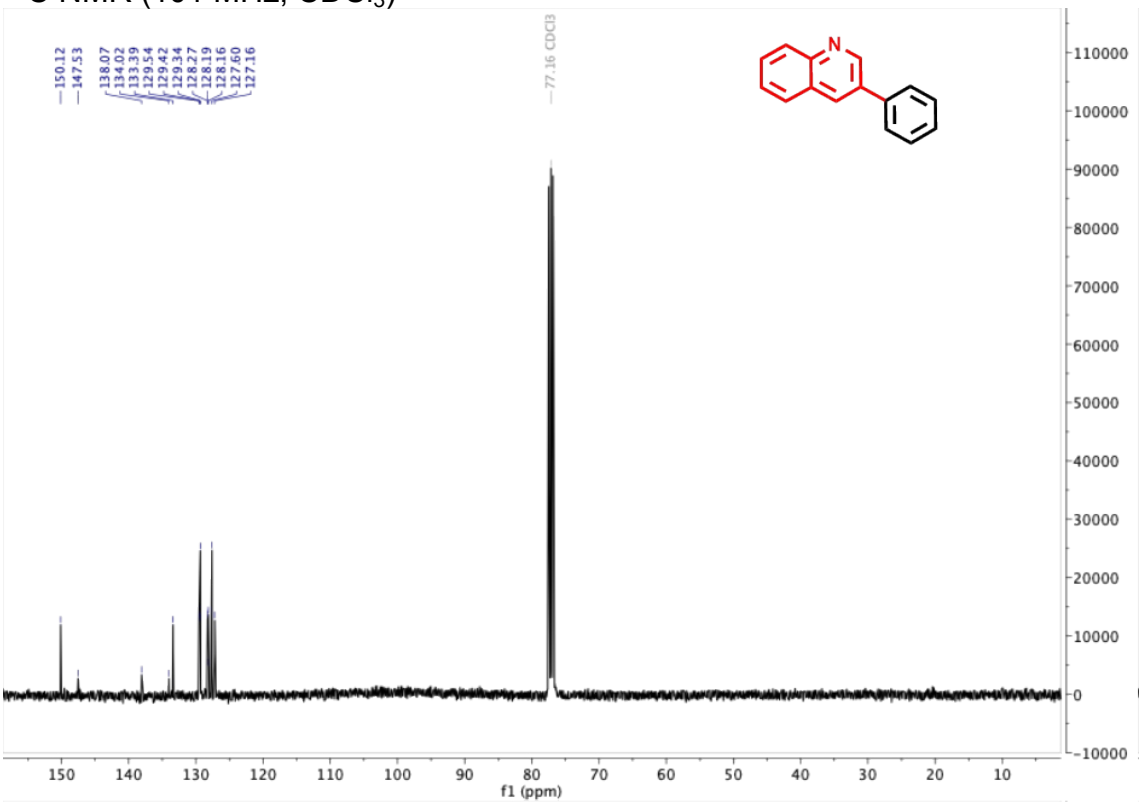

^{13}C NMR (101 MHz, $CDCl_3$)

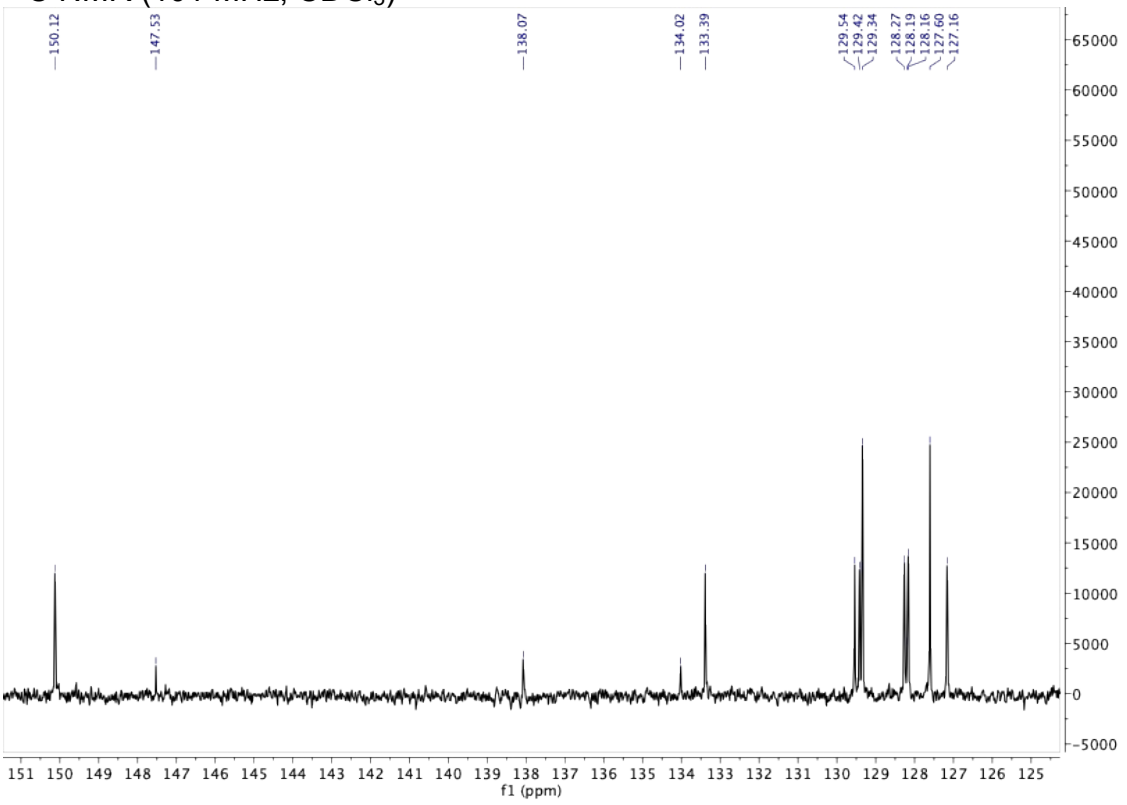

15. **References**

1 Park, K.; Park, S. S.; Yun, Y. H. *.J. Porous Mater.,***2017**, *24*, 1215–1225.

2 Xiao, J.; Lu, Z.; Li, Y. *Ind. Eng. Chem. Res*. **2015**, *54*, 790−797.

3 Ansari, T. N.; Sharma, S.; Hazra S.; Jasinski, J. B.; Wilson. A. J.; Hicks, Leahy, D. K. F.; Handa, S. *JACS Au* **2021**, *1,* 1506–1513.

4 Maegawa, T.; Kitamura, Y.; Sako, S.; Udzu, T.; Sakurai, A.; Tanaka, A.; Kobayashi, Y.; Endo, K.; Bora; U.; Kurita, T.; Kozaki, A.; Monguchi, Y. Sajiki, H.. *Chem. Eur. J*. **2007**, *13*, 5937–5943.

5 Yu, D.; Jie, B.; Wang, J.; Li, C. *J. Catal*. **2018**, *365*, 195-203.

6 Li, Y.; Xu, L.; Xu, B.; Mao, Z.; Xu, H.; Zhong, Y.; Zhang, L.; Wang, B.; Sui, X. *ACS Appl. Mater. Interfaces* **2017**, *9, 20*, 17155–17162.

7 Donga, Y.; Wua, X.; Chena, X., Wei, Y. *Carbohydr. Polym.* **2017***, 160*, 106–114.

8 Baran, N. Y.; Baran, T.; Menteş, A. *Carbohydr. Polym.* **2018***, 181*, 596–604.

9 Li, D.; Miao, F.; Chen, J.; Liu, Z.; Wang, Z.; Wang, Y. *Processes* **2025**, *13*, 339 (11 pages).

10 Zhu, Z.; Liang, S.; Sun, H.; Zhang, W.; Yang, J.; Gao, Z. *Catal. Sci. Technol*. **2024**, *14*, 3176-3183.

11 Liu, N.; Liu, C.; Jin, Z. *Green Chem*., **2012**, *14*, 592-597.

12 Li, X.; Liu, Y.; Zhang, L.; Dong, Y.; Liu, Q.; Zhang, D.; Chen, L.; Zhao, Z.; Liu, H. *Green Chem.*, **2022**, *24*, 6026–6035.

13 Bhadra, S.; Dzik, W. I.; Goossen, L. J. *J. Am. Chem. Soc.*, **2012**, *134*, 9938–9941.

14 John, M. E.; Nutt, M. J.; Offer, J. E.; Duczynski, J. A.; Yamazaki, K.; Miura, T.; Moggach, S. A.; Koutsantonis, G. A.; Dorta, R.; Stewart, S. G. *Angew Chem Int Ed*, **2025**, *64*, e202504108.